NRL Memorandum Report 1547

ILLUSTRATED GLOSSARY OF FRACTOGRAPHIC TERMS

SECTION 2

GLIDE PLANE DECOHESION
SERPENTINE GLIDE
RIPPLES
STRETCHING
MICROVOID COALESCENCE

C. D. Beachem and D. A. Meyn

METALLURGY DIVISION

June 1964

U. S. NAVAL RESEARCH LABORATORY
Washington, D.C.

ABSTRACT

The various fracture surface features formed by fine-scale plastic flow processes are discussed, and the mechanisms by which they are formed are discussed where they are known.

Glide plane decohesion, as it has been used in the literature, is shown to be misleading, and a more descriptive term, "stretching", is used in its place. The use of "ductile cleavage" to describe the same process should be discontinued.

The use of specific plastic flow mechanisms, such as cross-slip, twinning, wavy slip, pencil glide, and multiple slip to describe mechanisms responsible for the production of fracture surfaces should be reserved for those cases where the specific mechanism has been definitely established for a specific region of a specific fracture surface. Such definite identification of deformation mechanisms is seldom encountered in the electron fractography literature.

Since brief, descriptive, non-misleading terminology is necessary for immediate communication, several terms have evolved to describe the surfaces created by unknown processes. Glide plane decohesion, serpentine glide, ripples, stretching, and three kinds of microvoid coalescence are shown to be parts of a spectrum of plastic rupture - the

one end of the spectrum being slip on one or a few parallel planes to give separation of a large single crystal, and the other end of the spectrum being on too fine a scale for the mechanisms to be studied with present day replicas.

* * *

PROBLEM STATUS

This is an interim report; work on this problem is continuing.

* * *

AUTHORIZATION

NRL Problem Number M01-08
Bureau Project Number WW 041 [R05-24G]

INTRODUCTION

The metals and alloys which are tough owe this property to their ability to deform plastically and absorb energy before or during fracturing. The present report will describe the mechanisms responsible for three fracture modes involving extensive plastic deformation, insofar as these mechanisms have been worked out. All of these modes involve the same fundamental process, glide on one or more sets of crystallographic planes, but the resulting fracture topography is different and therefore different names are used for the various fracture appearances even though the basic process in each is the same.

The naming of fracture topographic features often reflects the concepts of the manner in which the features are generated. The features observed at the magnifications used in electron microscopy are produced by local stresses which, because of inclusions, voids, anisotropic grains in polycrystalline metals, etc., may be very different from the macro stresses imposed on the specimen. One is often forced, therefore, to infer not only the microfracture process but also the local state of stress which produced the local process.

FINE SCALE MECHANISMS

A. Glide Plane Decohesion

Single crystals of pure metal may, when pulled, glide apart along slip planes. When these crystals are large, the

slip along these planes is readily visible to the unaided eye. This process, if continued on the same plane, leads eventually to the specimen parting along a glide plane. This mode of separation, whether on a macroscopic or microscopic scale, and whether or not carried to completion, is appropriately called "glide plane decohesion" when the glide surfaces can be identified as such. It will be seen to be an important process in the fracturing of many alloys of practical usefulness.

B. Serpentine Glide

Particularly in polycrystalline metals where the deformation of a given grain must accommodate to the deformation of its neighboring grains, gliding may occur on many sets of intersecting planes and in an irregular manner giving rise to a pattern which has come to be known as "serpentine glide". Serpentine glide surfaces, then, are formed by (partial) glide plane decohesion on several sets of planes by unspecified mechanisms, giving a particular interwoven or plaited appearance on the fracture surface. This will be illustrated in several subsequent electron fractographs.

The sketch in Fig. 1 shows the idealized stress pattern at a free surface at the root of a notch or crack (or any other free surface) in a stressed specimen. Fig. 2 is a further consideration of the stresses at a free surface. Here we are viewing the stressed element along the intersection

of the local planes of maximum shear stress, i.e., along the direction of σ_2. Though glide need not occur on planes of maximum shear stress, localized glide is shown here along one family of planes of maximum shear stress producing steps which may also be seen in an actual case in Fig. 3a. This specimen was an ingot iron wire 1/8" in diameter, notched with a file perpendicular to the axis of the wire. The root of the notch was caused to open by bending the wire as shown in the sketch in Fig. 3b. The features indicated at A and B in Fig. 3a are serpentine glide, and such surfaces may be seen in stereo viewing to be stepped as in Fig. 2. The light surfaces marked by B's (Fig. 3a) are the new free surfaces created by plastic flow on glide planes - glide plane decohesion. If further glide takes place either on other planes in the same set or on planes in other sets, the markings tend to be smoothed out - becoming first "ripples" (1) [as seen at C in Fig. 3a] and then featureless as the glide steps become too small to be shown by the fidelity of present day replicas. These events are sketched in Fig. 4, and are apparent in Fig. 3a when one realizes that the sharp step-like markings of serpentine glide are at the bottom of the trough where plastic flow is in the early stages and that the ripples are smoother near the file marks where additional glide has taken place.

Such glide markings as are visible in Fig. 3a and others throughout this report can in general be formed by a combination of such elementary slip mechanisms as pencil or wavy slip (2,3,4), irregular slip, and cross and multiple slip. Two of these are illustrated in Fig. 5. It is likely that multiple slip will operate independently of the other mechanisms and increase the general complexity of the surface appearance.

C. Stretching

When glide produces new surfaces in heavily cold-worked metal, the glide planes are poorly defined and the glide steps may be so poorly delineated (at least in replication processes now available for fracture surfaces) that the new surface may appear featureless. The term which has been used for the processes which generate such surface areas is "stretching", which is then glide plane decohesion carried so far that the glide marks are no longer seen. As the glide steps become so small that they cannot be seen in replicas, they approach the dimensions of dislocations that permit glide, and further deformation at the free surface must be by some highly complicated dislocation entangling process which makes the local metal seem to behave more like a highly ductile amorphous material than a crystalline material.

An experiment which illustrates the fact that these smooth featureless surfaces are formed by stretching rather

than by "glide plane decohesion" or "ductile cleavage" is illustrated in Figs. 6-9. A piece of annealed 99.999% pure copper wire was notched and the wire was bent to open the root of the notch. After palladium was evaporated into the notch, the wire was bent some more and carbon was evaporated into the notch. This direct carbon replica was then freed from the specimen and studied. Fig. 6 shows a portion of the root of the notch which was only slightly stretched in the direction of the arrows after the palladium was evaporated. Fig. 7 shows a region where additional stretching was more extensive on one side than on the other. The right-hand side of the picture shows such extreme stretching that one cannot tell in which direction it was stretched. Good examples of serpentine glide surfaces may be seen in Figs. 8 and 9 where the plastic flow, or glide, processes have not been carried to the extreme of stretching. Fig. 8 shows where this process has crossed three boundaries, including two that apparently are the boundaries of an annealing twin. It is interesting to notice that these regions (Figs. 8 and 9) do not show any palladium. This means that some of the most recently exposed free surfaces are in the early stages of growth. From this observation, one might expect to find mixtures of stretching, glide plane decohesion, and serpentine glide simultaneously acting in neighboring regions of a deforming specimen, with

the process depending upon the number of grains in the specimen, their orientation, and the degree of deformation at the time when the replica is taken.

Another example of the stretching process is shown in Fig. 10. In this as-cast Ti-2Al-2Zr-2V-1Mo alloy, a sheet of an unknown constituent is seen to be broken up into segments which have moved apart by stretching of the bulk material in the directions shown by the arrows.

Thus stretching, which is by no means an accurate description of the basic plastic flow mechanisms, is a much more descriptive and much less misleading term than glide plane decohesion or ductile cleavage.

Stretching is defined as the production of smooth featureless free surfaces by extremely complex plastic flow mechanisms localized in volumes of material too small to produce characteristic surface traces in present day replicas.

D. Microvoid Coalescence

Small particles of precipitate, undissolved carbides, sulfides, silicates, oxides, or other brittle or weak constituent particles are frequently present in large numbers in all but the purest of metals. When the metal around these particles is plastically deformed these particles often create internal free surfaces by either cleaving or separating from the adjacent metal along the interfaces.

Under plastic strain these free surfaces nucleate voids which grow by plastic rupture processes similar to those at the root of the opening notch in Fig. 3. With extreme plastic growth of voids (voids frequently grow one or two orders of magnitude larger than the free surfaces that initiate them), steps or ripples are visible only rarely in present-day replicas, particularly in high-strength alloys. In addition, the spherical or rounded shape of the voids prohibits simple glide: Slip must occur in a highly complex manner in the severely worked material on the surface of the void (hundreds or thousands of percent elongation - if we care to visualize plastic deformation on this scale in this manner) during the growth of a spherical or rounded internal void.

The voids which are nucleated at some sort of metallurgical singularity grow under plastic strain by the glide processes which have been termed "stretching" above. (Growth by diffusion of vacancies is too slow a process.) A void may grow until it impinges on a neighboring void under one of three stress configurations as depicted in Fig. 11. When voids impinge and the last remaining metal separates under normal stress, the newly opened surface can be shown to consist (on both fracture faces) of a cuplike depression which has come to be called an equiaxed dimple (or sometimes a cupule), and the process has come to be called "normal dimpled rupture".

If, however, the voids grow and coalesce under shear stresses, as in the second series of Fig. 11, they are elongated in the shearing direction. The surface of the shear fracture shows the elongated dimples with one end continuous and the other end "stretched out" until that end appears open. Observations on precisely matched fracture sites have confirmed that one set of "shear dimples", as these are called, points toward the origin of the shear fracture and the set on the other fracture surface points in the opposite direction. To date no features have been found which could be used to determine, by looking at the dimple, in which direction the shear crack front moved.

If voids grow and coalesce under a bending moment, as in the third sequence of Fig. 11, they also are elongated, and when observed on only one fracture surface they are indistinguishable from shear dimples. But the dimples on the matching surface in this case are "pointing" in the same direction as on the other half, and on both fracture surfaces they point toward the fracture origin. These have been termed "tear dimples" since they have been generated by a tearing action.

It will be seen that these three forms of surfaces created by microvoid coalescence - equiaxed, shear, and tear dimples - may sometimes appear in close proximity in what appears macroscopically to be a surface of a single fracture

mode. This is attributed to the metallurgical heterogeneities mentioned earlier or to transients in the stress pattern.

FRACTOGRAPHS FURTHER ILLUSTRATING PLASTIC RUPTURE SURFACES

Metals that are soft and sufficiently free from precipitate particles, inclusions, etc. tend to favor failure by glide plane decohesion and its extensions serpentine glide and stretching. In addition to Fig. 3a, Figs. 12-15 show fracture surfaces created by this mode. The serpentine glide surfaces in Figs. 12 and 13 might be mistaken by the unwary doing a failure analysis for fatigue markings. The occasional crossing of the glide markings (e.g., between the arrows) however, may often be used to identify these as serpentine glide surfaces rather than fatigue surfaces.

Figs. 3a and 13 (arrows) also show isolated dimples which nucleated near the stretching surface, grew to the surface, opened, and stretched out in the surface. In Fig. 3a the stretching of the dimple in the surface is so extensive that its two separated ends are not easily recognized as mates. Figs 15 and 16 show increasing numbers of dimples in stretched surfaces while Figs 17-19 are composed entirely of dimples. Thus a full spectrum is seen, ranging from no dimples to all dimples on a stretched surface. Fig. 17 clearly shows serpentine glide in many of the dimples.

Surfaces formed by the tearing mode of microvoid coalescence are illustrated in Figs. 17-19. (Figs. 13, 15, 16, 18,

and 19 show both ends of oval dimples in a stretched surface where it is obvious that the dimples grow by an "opening" mode and are therefore by definition tear dimples.) Most of the tear dimples in Figs. 18 and 19 could be identified only by checking the directional sense of the dimples on the matching fracture surface.

The tear dimples shown in Fig. 19 were observed in a replica from the center of a cup-and-cone tensile failure surface in a 282,000 UTS AISI 4340 smooth bar specimen. The two halves of the specimen are shown in Fig. 20 while the fracture initiation region is shown in Fig. 21 at a higher magnification. The fracture started at a small diameter (but deep) "pinhole" by radial tearing. Tearing proceeded about 1/10 the specimen diameter before it changed to mixed tearing, shear rupture, and normal dimpled rupture.

Examples of surfaces formed by normal dimpled rupture are seen in Figs. 17, and 22-25. Normal dimpled rupture is a mode often operative in running "brittle fractures" of high-strength steels and aluminum alloys. This fracture mode is almost always accompanied by other regions fracturing by shearing or tearing.

Examples of surfaces formed by shear rupture are seen in Figs. 26-30. Precisely matched shear dimples are shown in Figs. 29 and 30 with the matching dimples marked with arrows.

In the shear dimple area of Figs. 29 and 30 there is an area of quasi-cleavage (5), and it may be noted that matching shear dimples adjacent to the quasi-cleavage are not of the same size or length. This effect extends for several microns up the shear lips. The sketch in Fig. 31 explains why the matching dimples are not of equal length. This effect has been observed also in AISI 4340 steel crack propagation specimens, where the boundary between the flat fracture and the shear lip is well delineated. The effect is difficult to recognize in smooth tensile specimens and in crack propagation specimens when the flat fracture is composed of dimples - both conditions give rise to greater plastic flow and thereby produce a less sharply defined boundary.

Tear dimples form frequently when voids coalesce with larger free surfaces. Low magnification photographs of a rubber-band model are shown in Fig. 32 for comparison with the oval tear dimples in Figs. 13, 15, 16, 18, and 19, and an explanatory sketch of the process is shown in Fig. 33. The model is shown only to indicate, in a simple manner, the stretching of this type dimple after the void has coalesced with the surface. Successive replicas from progressively stretched dimples at the bottom of notches in iron wire have confirmed this process in metal.

Another repeatedly observed feature of void coalescence and stretching is shown in Figs. 34-36. Sharp fatigue cracks are frequently used as stress raisers in crack propagation fracture toughness evaluations. Invariably, if the specimen does not cleave, stretching will occur at the tip of the crack when it is opened up in testing as indicated by Fig. 34. Initial failure by void coalescence cannot occur because (1) the lack of a third stress component at the free surface, or (2) the material at the tip of the crack has not been sufficiently deformed to grow voids. After a finite amount of growth by stretching, the crack usually intersects increasing numbers of voids as it grows through increasingly strained material, and tear dimples are formed as in Figs. 34-36. As the crack grows further - through material contained in an increasingly larger plastic zone - patches of voids open up and coalesce ahead of the crack and the fracture is seen to increasingly consist of random mixtures of tear dimples, shear dimples, and equiaxed dimples as seen in Fig. 34.

As mentioned in reference 6 the length of shear dimples depends upon the value of the ratio of normal (perpendicular to the shear plane) strain to shear strain in the material surrounding the voids during growth and coalescence of the voids. Dimple length increases as the value of the ratio

decreases. As the normal strain approaches zero the dimples are observed to be very long - five to ten times as long as they are wide (Fig. 37). Another effect of reducing the normal strain to zero is that when the specimen does shear apart at tiny local points, the two rupture surfaces may rub against one another as they separate. Where void coalescence markings end and burnishing markings begin has not been established yet, but both will consist mainly of long parallel lines (as in Fig. 38) - and neither of the markings indicate glide plane decohesion. To illustrate the complexity of distinguishing between initial rupture surfaces and burnishing markings, Fig. 39 shows rupture dimples where two mechanically polished pure copper surfaces were lightly rubbed together. These dimples were formed during rupture after local friction-welding occurred.

SOME FRACTOGRAPHIC TERMS NOT RECOMMENDED

If a metal specimen separates by glide plane decohesion, particularly if this is along only a few members of one set of crystallographic planes, the fracture surface consists largely of facets of one or at most a few specific lattice planes, and in this respect the fracture surface might be considered akin to cleavage, which also occurs on only one or at most a few crystallographic planes. It is understandable then why the process might be called "ductile cleavage" (ductile because extensive glide precedes fracture). This

is considered a less suitable term than glide plane decohesion and is not used in NRL reports on fractography.

The term "ductile rupture" has been used in the past for the process which has been termed in this report microvoid coalescence. Although some of the most ductile metals and alloys fracture by this mode, so do some of the alloys having very low engineering ductility (though the dimples tend to be much shallower in this case). It is felt that the term "ductile rupture" might suggest to the mechanical metallurgist greater toughness than a given alloy may possess, and accordingly "ductile rupture" has been dropped in favor of microvoid coalescence.

It is further recommended that the use of the term "glide plane decohesion" be discontinued in cases where glide planes are not distinctly visible, and the featureless surfaces created by unidentified processes of extreme plastic deformation be called "stretched" surfaces, and the mechanism called simply "stretching".

SUMMARY

Fine scale plastic flow processes are seen to be basically the same regardless of the features produced. Early stages of plastic deformation in soft crystals produce stepped free surfaces by glide plane decohesion. If these steps form an interwoven pattern, the process is called

serpentine glide. If the steps are further smoothed out the surface features are called ripples. If the process is carried far enough, smooth featureless surfaces are formed. These featureless surfaces grow under further deformation by an unidentified mechanism (or mechanisms) called stretching.

Depending upon whether or not internal microvoids are opened up, and their number, the stretched surfaces may or may not contain dimples, and the number of dimples will depend upon the number of microvoids intersected by the stretching surface. If a lot of microvoids are present, the fracture may progress by the microvoid coalescence process, rather than by stretching. Three distinctly different types of microvoid coalescence mechanisms have been observed - normal dimpled rupture, shear rupture, and tearing. Tearing dimples are found usually at the beginnings of fracture where fracture initiates at a sharp crack or internal flaw. A macroscopically flat "brittle" fracture surface may contain scattered patches of the three different types of fracture.

The mechanisms of stretching operate on a scale usually much smaller than the dimple size and no difference is suspected between the mechanisms underlying the growth of dimples and stretched surfaces.

Tear dimples, if both halves remain on one surface, appear as ovals or the ovals may be stretched open to the extent that the ovals become divided into two quasi-parabolic dimples.

ACKNOWLEDGEMENTS

The authors extend their thanks to Dr. B. F. Brown of the U. S. Naval Research Laboratory, Mr. E. P. Dahlberg at the University of Florida, and several members of the ASTM Sub Committee on Electron Fractography and Microstructures for their interest, help, and constructive criticism during the formulation of the terminology discussed in this report.

REFERENCES

1. Rogers, H. C., "Tensile Fracture of Ductile Metals", Trans AIME 218:498, Jul 1960.
2. Barrett, C. S., "Structure of Metals", McGraw-Hill Book Co., p. 340 (1952).
3. Crussard et al., "A Comparison Between Ductile and Fatigue Fracture", Swampscott Conference on Fracture, p. 19-21 (1959).
4. Cottrell, A. H., "Dislocations and Plastic Flow in Crystals", The Oxford University Press, p. 4 (1953).
5. Beachem, C. D., Brown, B. F., and Edwards, A. J., "Characterizing Fractures by Electron Fractography, Part XII. Illustrated Glossary, Section 1: Quasi-Cleavage", NRL Memorandum Report 1432, Jun 1963.
6. Beachem, C. D., "An Electron Fractographic Study of the Influence of Plastic Strain Conditions Upon Ductile Rupture Processes in Metals", Trans ASM 56[3], Sep 1963.

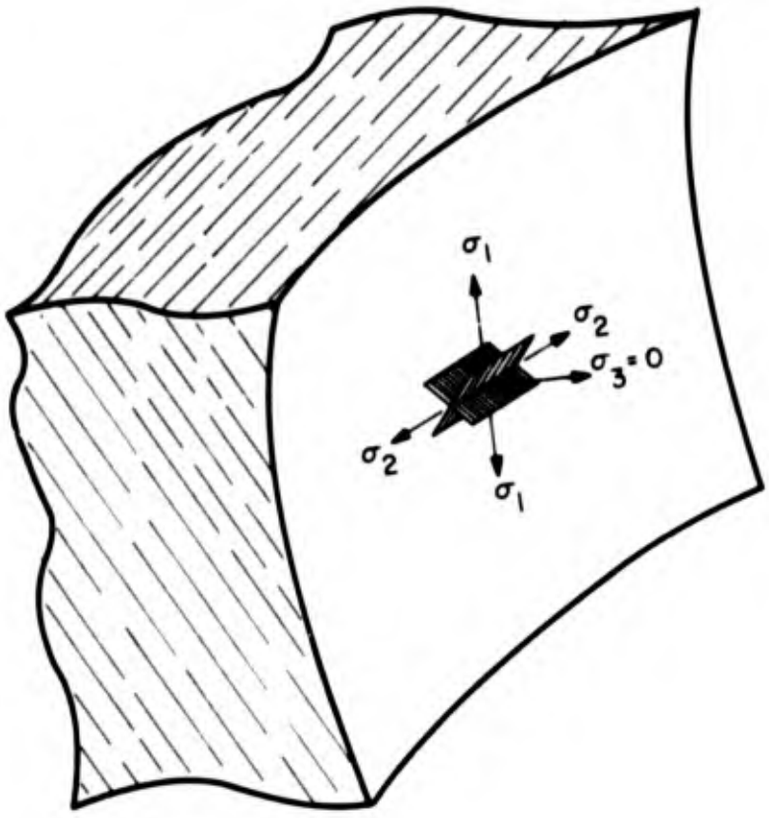

Fig. 1 - Stress configuration at a free surface where the local maximum principal stress is vertical. The shaded planes are the local planes of maximum shear stress.

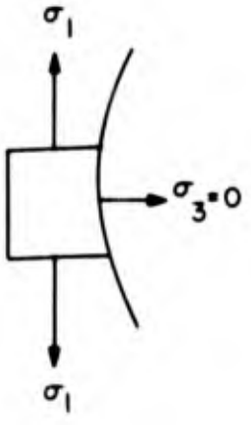

A. BEFORE GLIDE

B. AFTER GLIDE ON A SERIES OF PARALLEL PLANES THAT ARE FAVORABLY ORIENTED FOR GLIDE

Fig. 2 - Simplified general model for the creation of a rupture or fracture surface by a simple glide process. Though glide by a slip process is shown, glide by twinning may also produce new free surfaces. Arrows indicate the new (rupture, fracture) surfaces, created by glide plane decohesion.

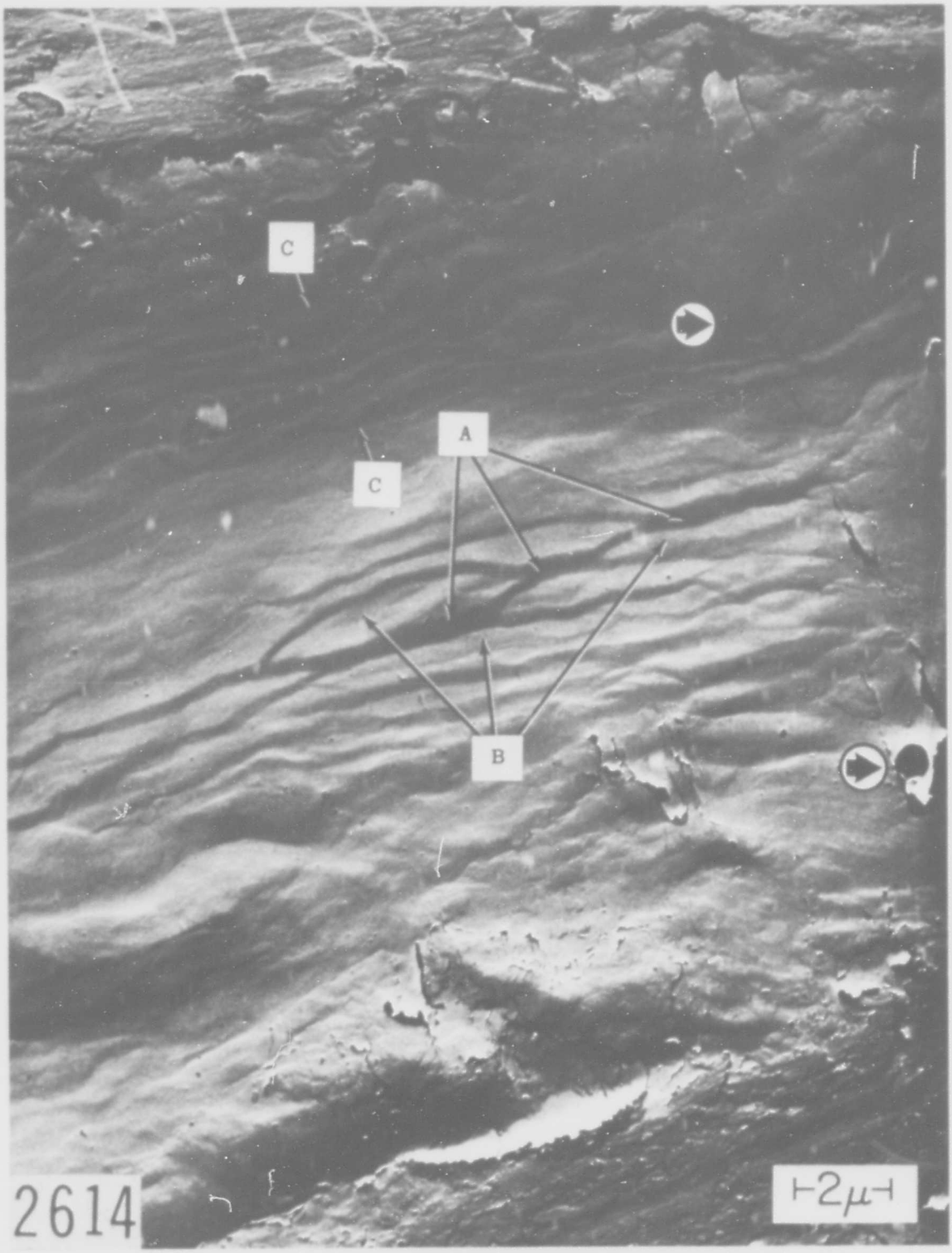

Fig. 3a - Serpentine glide surface in annealed Armco iron. This glide was probably produced by wavy slip when the root of a notch in this wire specimen was opened up by bending at room temperature. The dark surfaces (A) apparently were a single surface before slip on a second series of parallel planes produced the light parallel surfaces (B). Examples of ripples may be seen between the C arrows. Palladium shadowed direct carbon replica. 9000X.

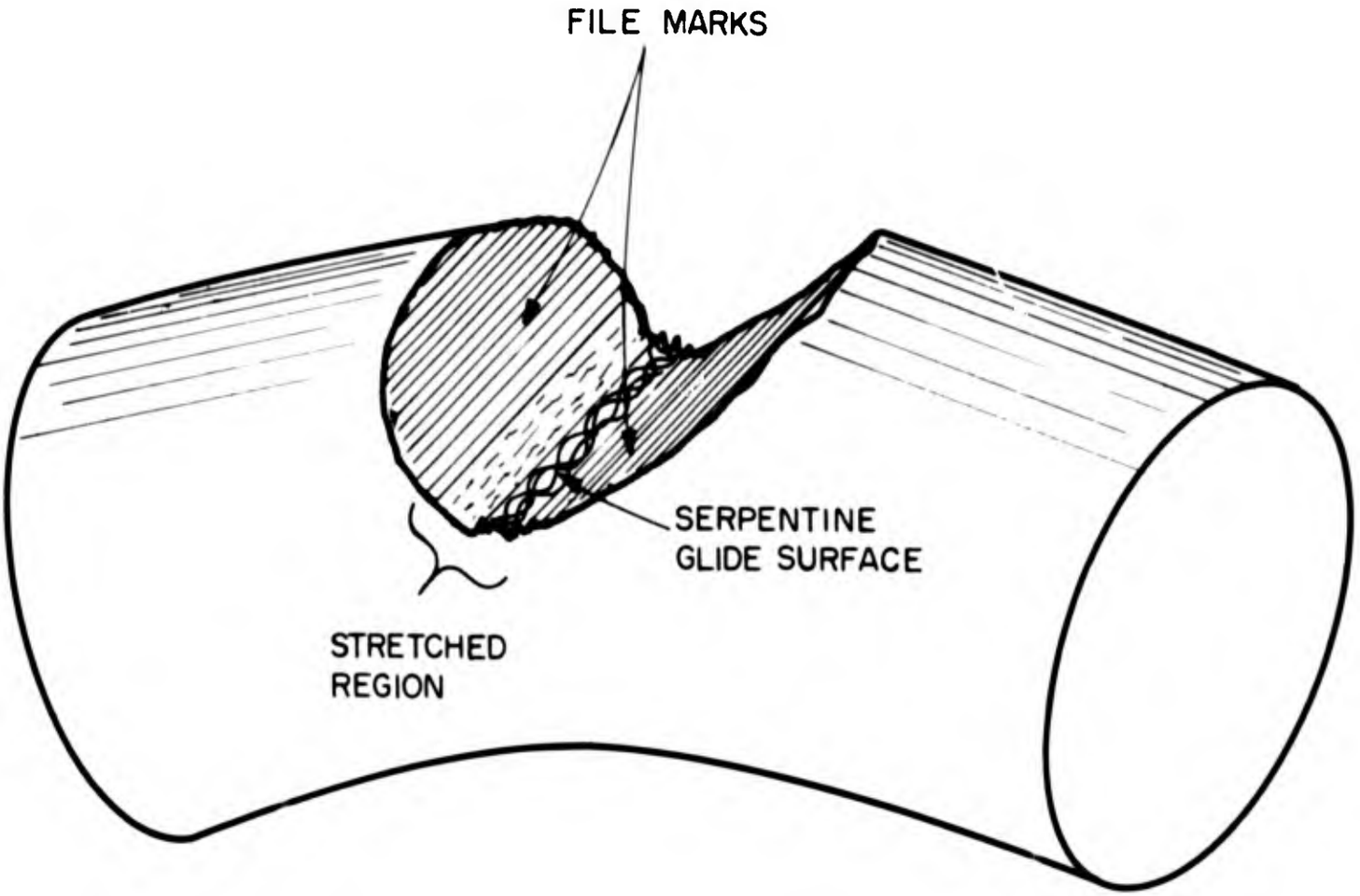

Fig. 3b - Sketch of wire specimen from which replica shown in Fig. 3a was taken.

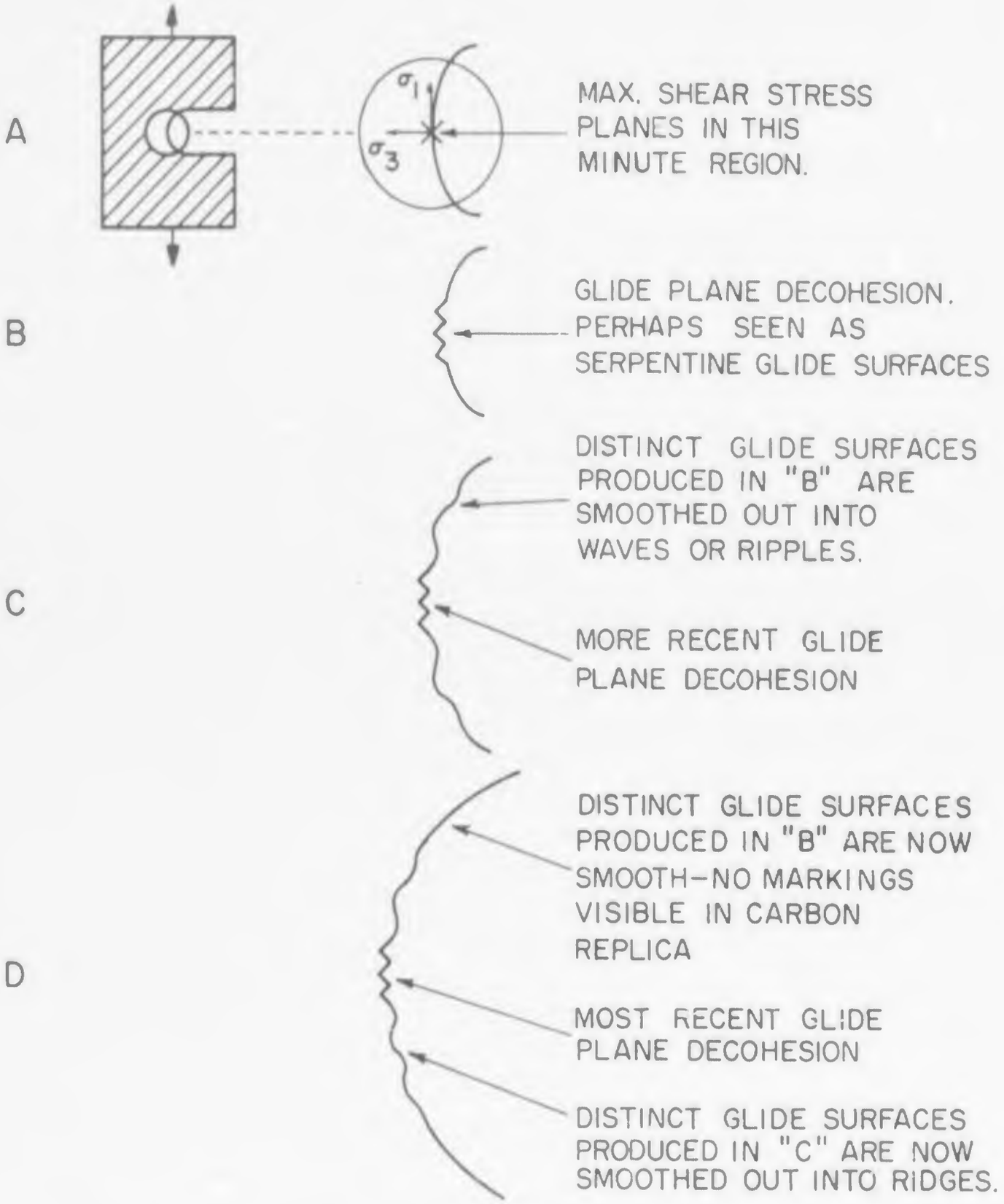

Fig. 4 - The production of smooth surfaces by plastic flow. Surfaces definitely produced by glide plane decohesion are smoothed by severe plastic deformation – stretching – until no markings are visible on ordinary replicas. Elongation is vertical, and increases from top to bottom. Crack propagation direction is from right to left.

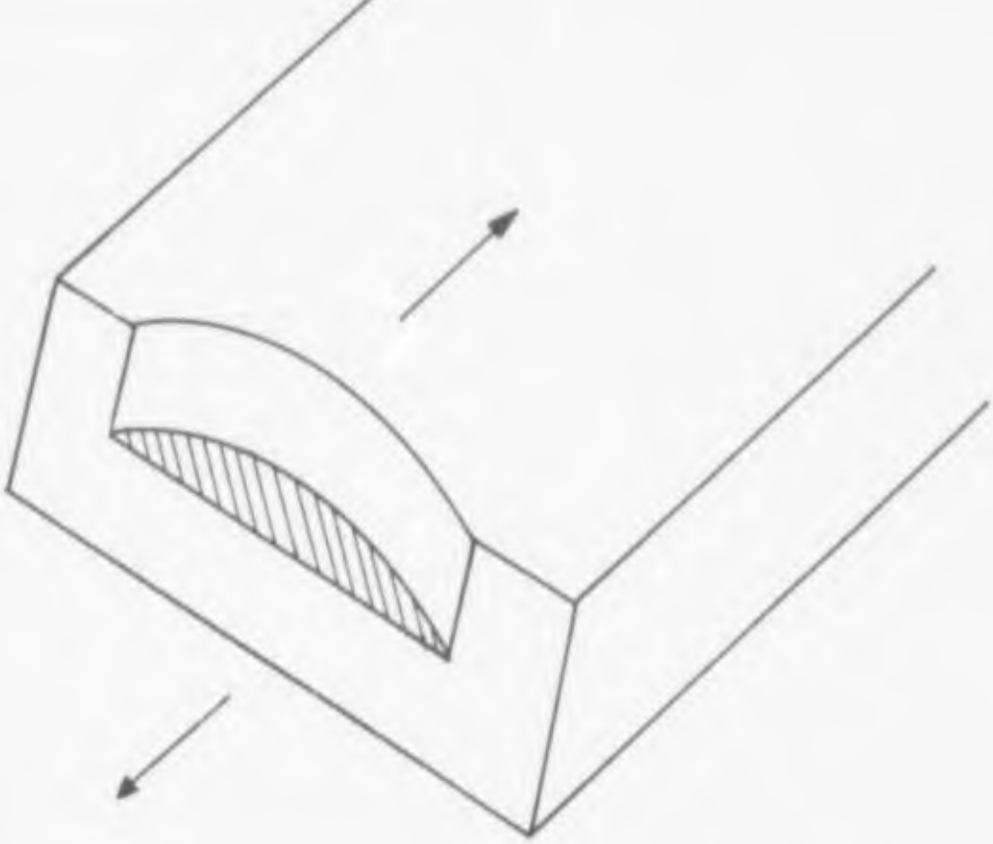

Fig. 5a - Irregular slip. Slip intersects the surface in irregular fashion, producing irregular slip steps (cross-hatched). This is very similar to some features actually seen in Figs. 3a and 12.

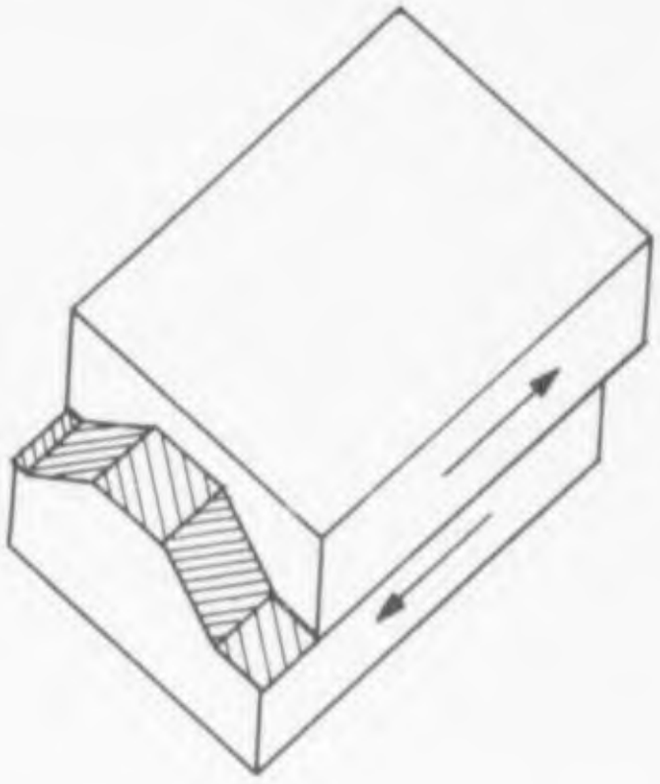

Fig. 5b - Pencil slip, also called wavy slip or wavy glide in α-iron by Barrett (2). Cross-slipping screw or multiplanar edge dislocation can create this appearance. Resulting slip step is cross-hatched. From Cottrell (3).

Fig. 6 - Stretching at the root of a notch in a 99.999% pure Cu wire specimen. Stretching occurred in directions of the arrows after the Pd was deposited, and before the carbon was deposited. Dark areas are Pd, light areas are newly stretched. Direct carbon replica. 6000X.

Fig. 7 - Extensive stretching in 99.999% Cu after the deposition of Pd. Direct carbon replica. 9000X.

Fig. 8 - Serpentine glide in 99.999% Cu. Direct carbon replica. No shadow. 9000X.

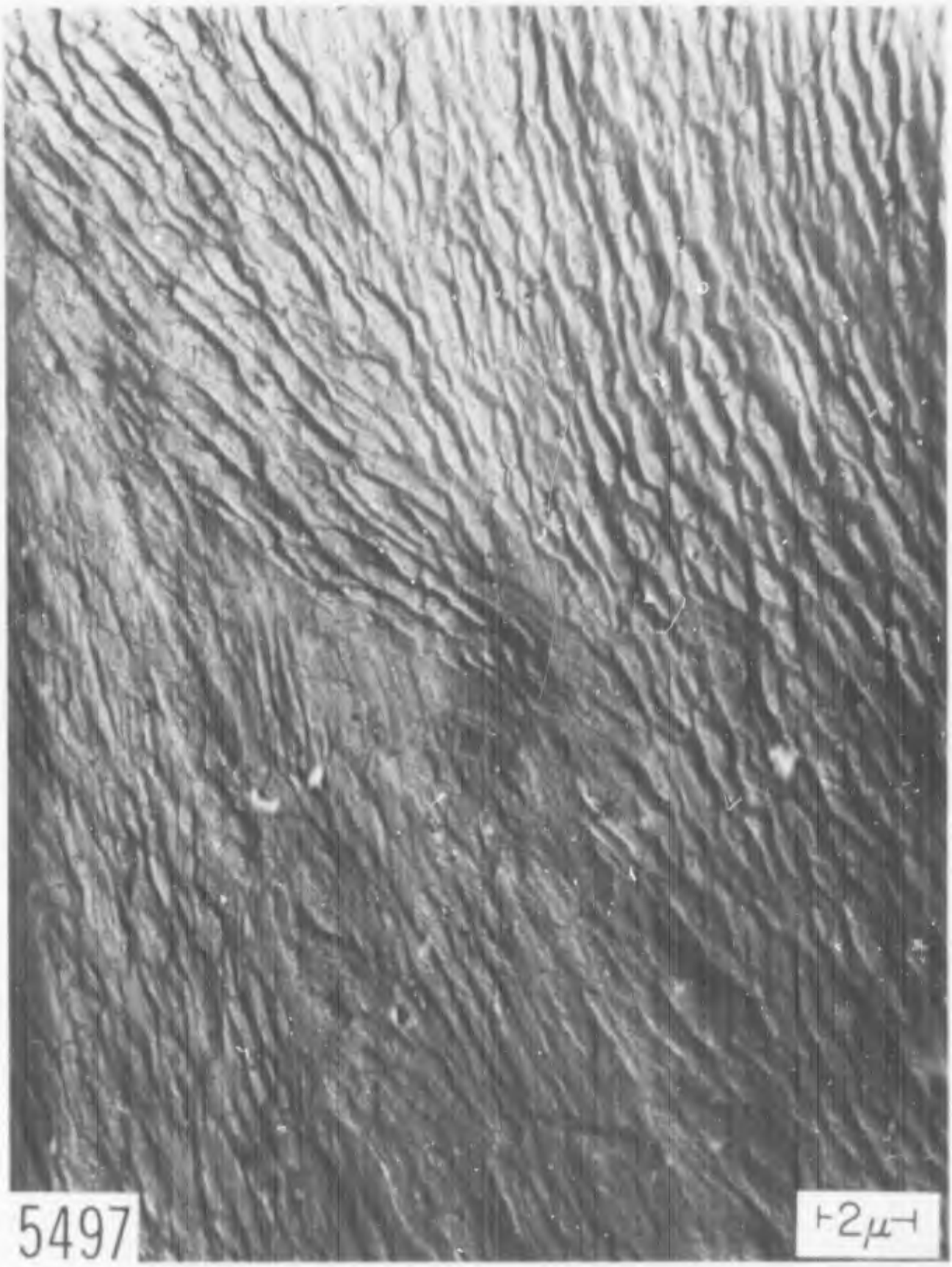

Fig. 9 - Serpentine glide in 99.999% Cu. Direct carbon replica. No shadow. 9000X.

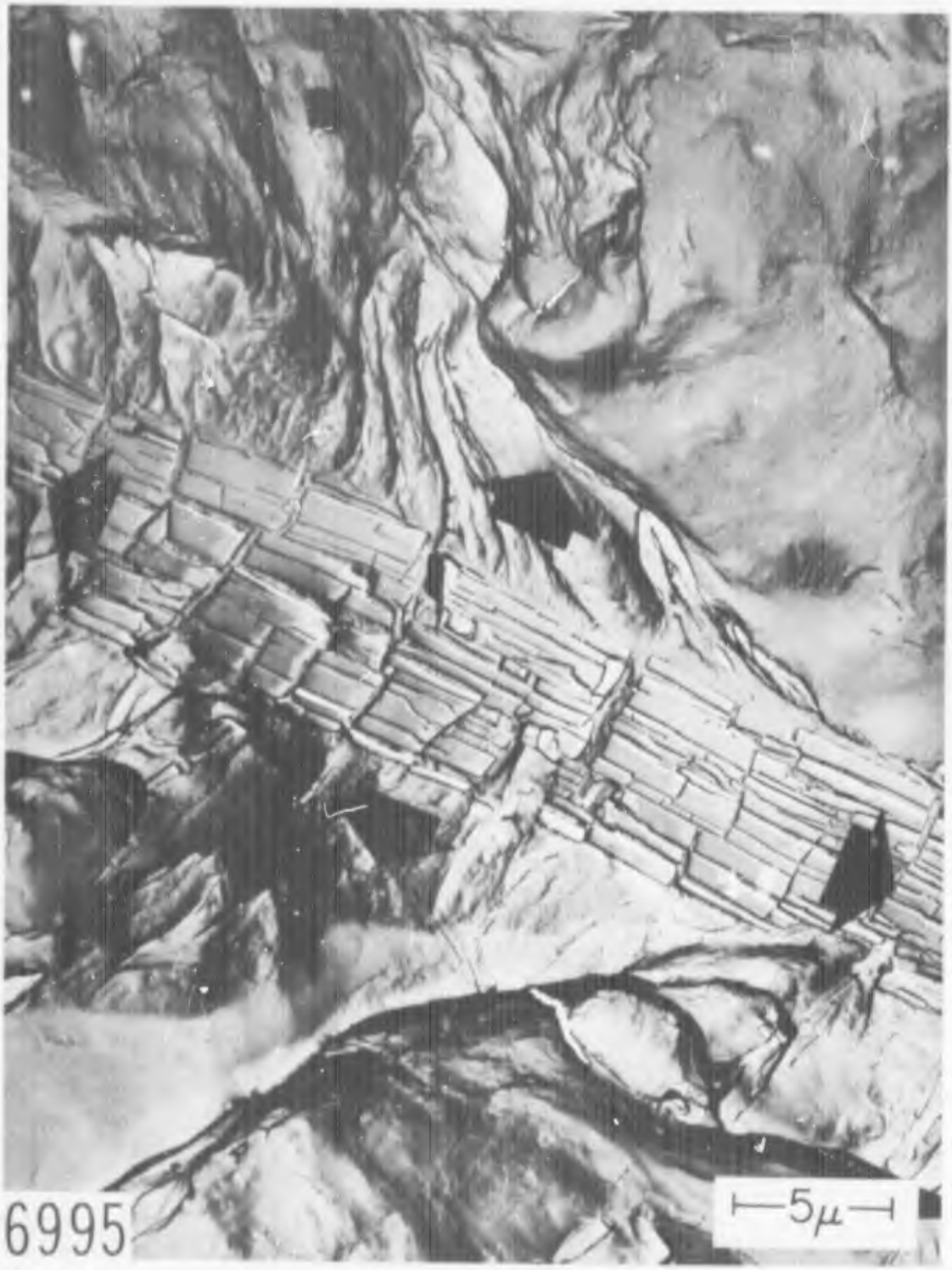

Fig. 10 - Stretching in as-cast Ti-2Al-2Zr-2V-1Mo. The flat constituent particles have been expanded in two directions (arrows) on a relatively flat area as a result of stretching of the underlying metal. Surrounding metal is much more severely stretched. Two-stage carbon replica. 6000X.

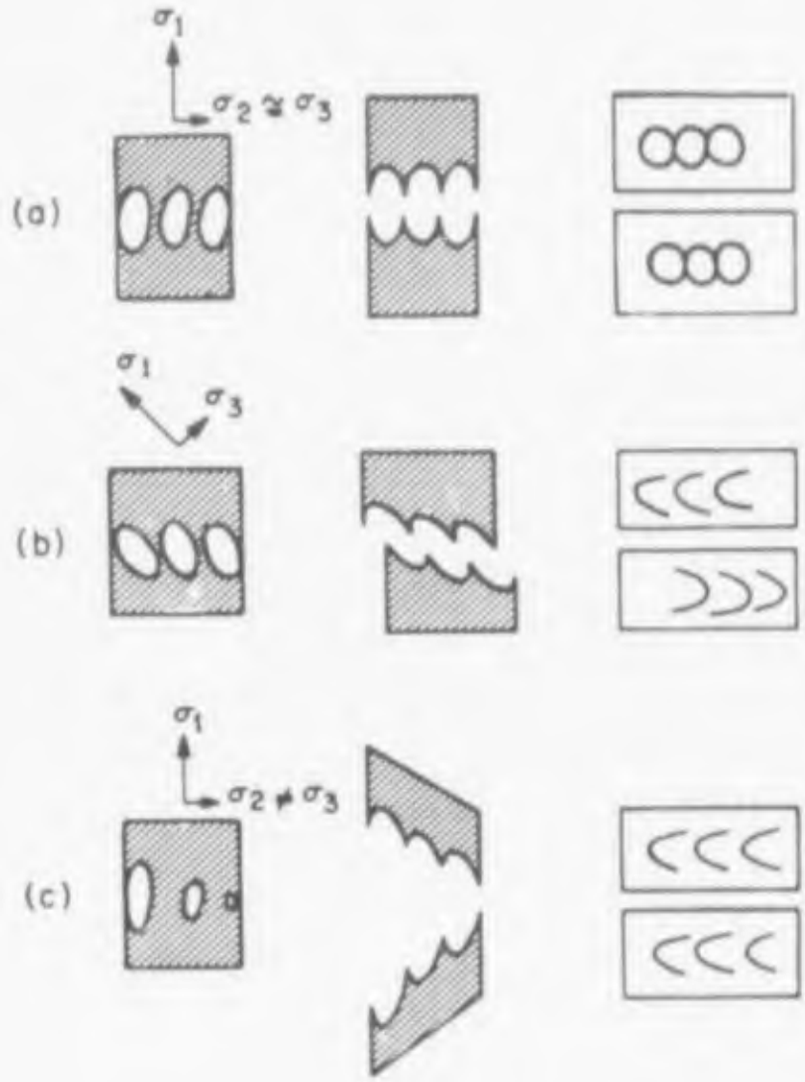

Fig. 11 - Three observed basic modes for the coalescence of microvoids. For each mode the sketches show from left to right: material stressed almost to the point of local rupture; local rupture, and the directional sense of dimples on the rupture surfaces. The three coalescence modes are called: (a) normal dimpled rupture; (b) shear rupture, and (c) tearing.

Fig. 12 - Serpentine glide in Armco iron. Distinct glide steps, created by glide plane decohesion, are seen between the arrows. Palladium-shadowed two-stage carbon replica. 6000X.

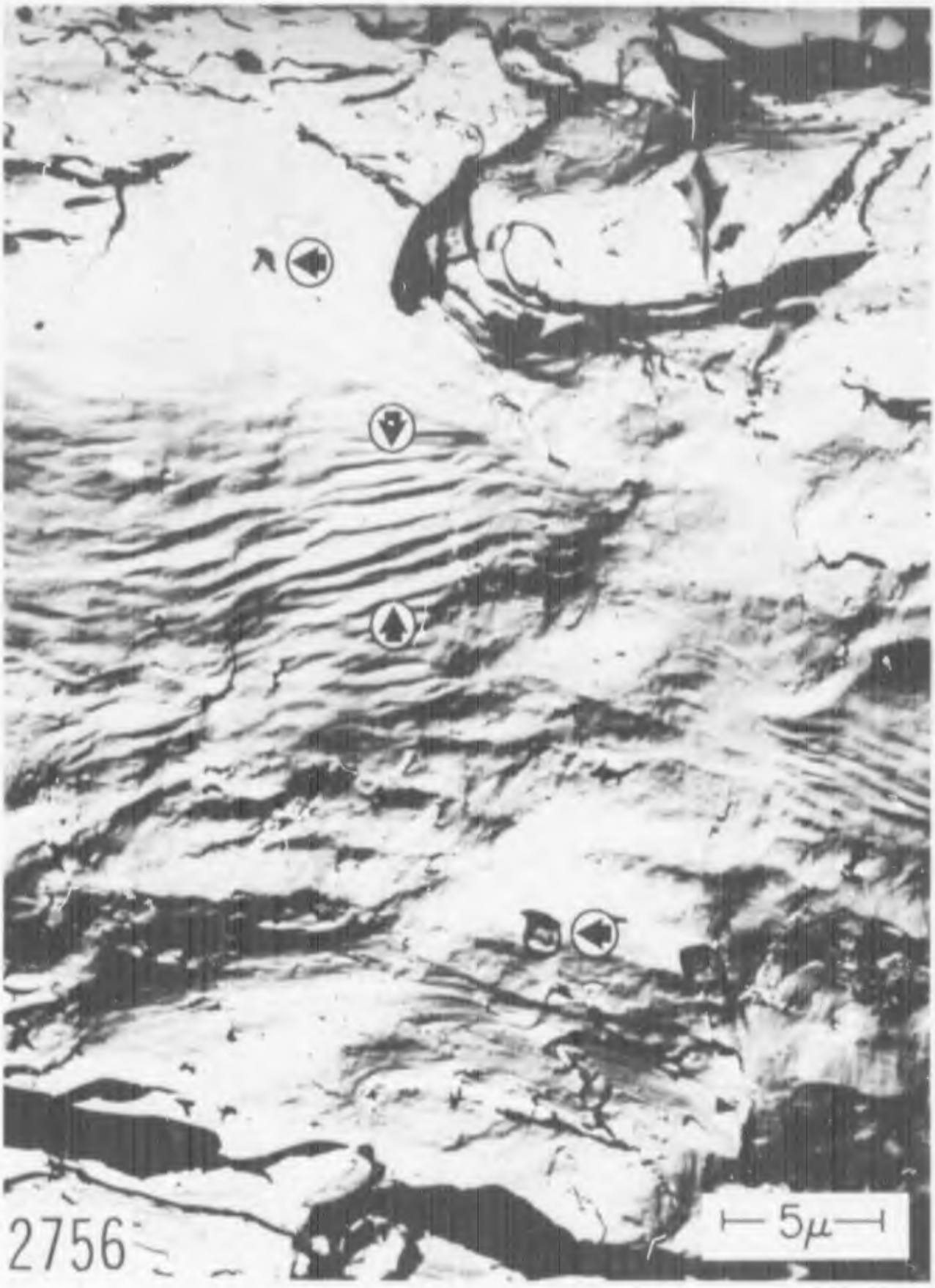

Fig. 13 - Serpentine glide in Armco iron. Two dimples are indicated by horizontal arrows. The glide plane decohesion steps between the vertical arrows were probably formed by duplex slip. Palladium-shadowed two-stage carbon replica. 6000X.

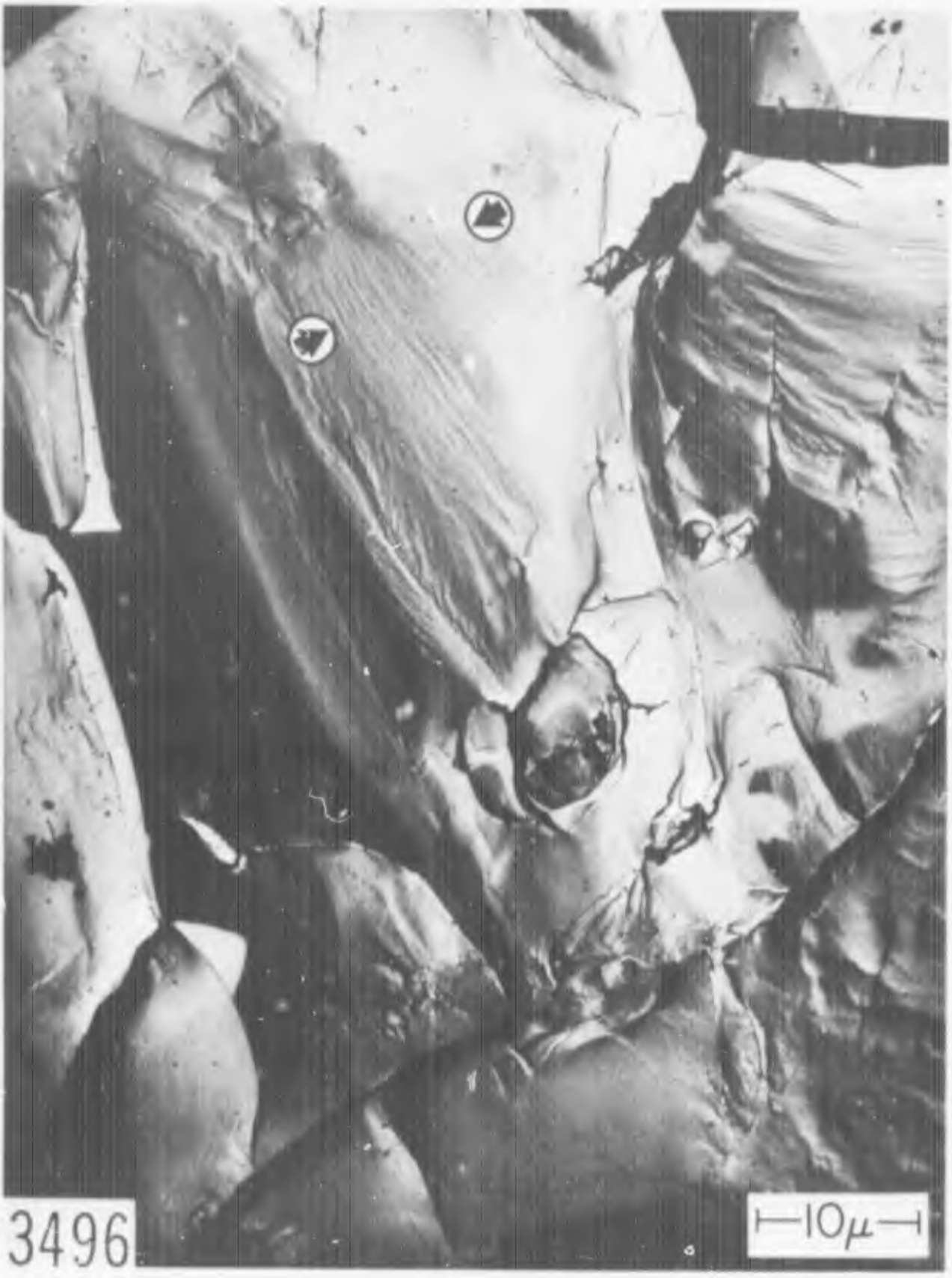

Fig. 14 - Serpentine glide (example between arrows) and stretching in unalloyed annealed Ti. Two-stage palladium-shadowed replica. 3000X.

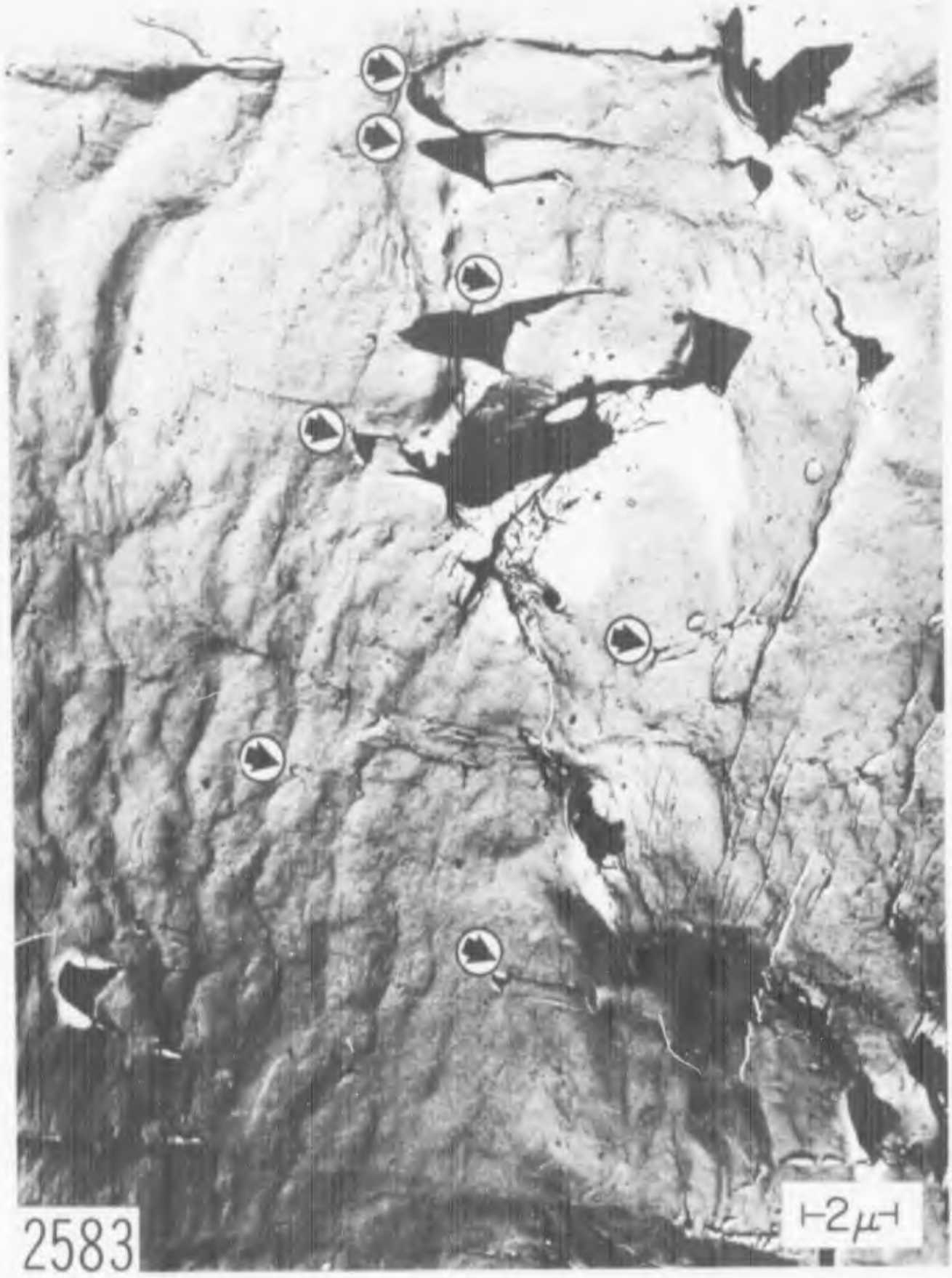

Fig. 15 - Ripples (lower left 1/4 of fractograph), stretching and oval tear dimples (arrows) in Armco iron. Two-stage palladium-shadowed carbon replica. 9000X.

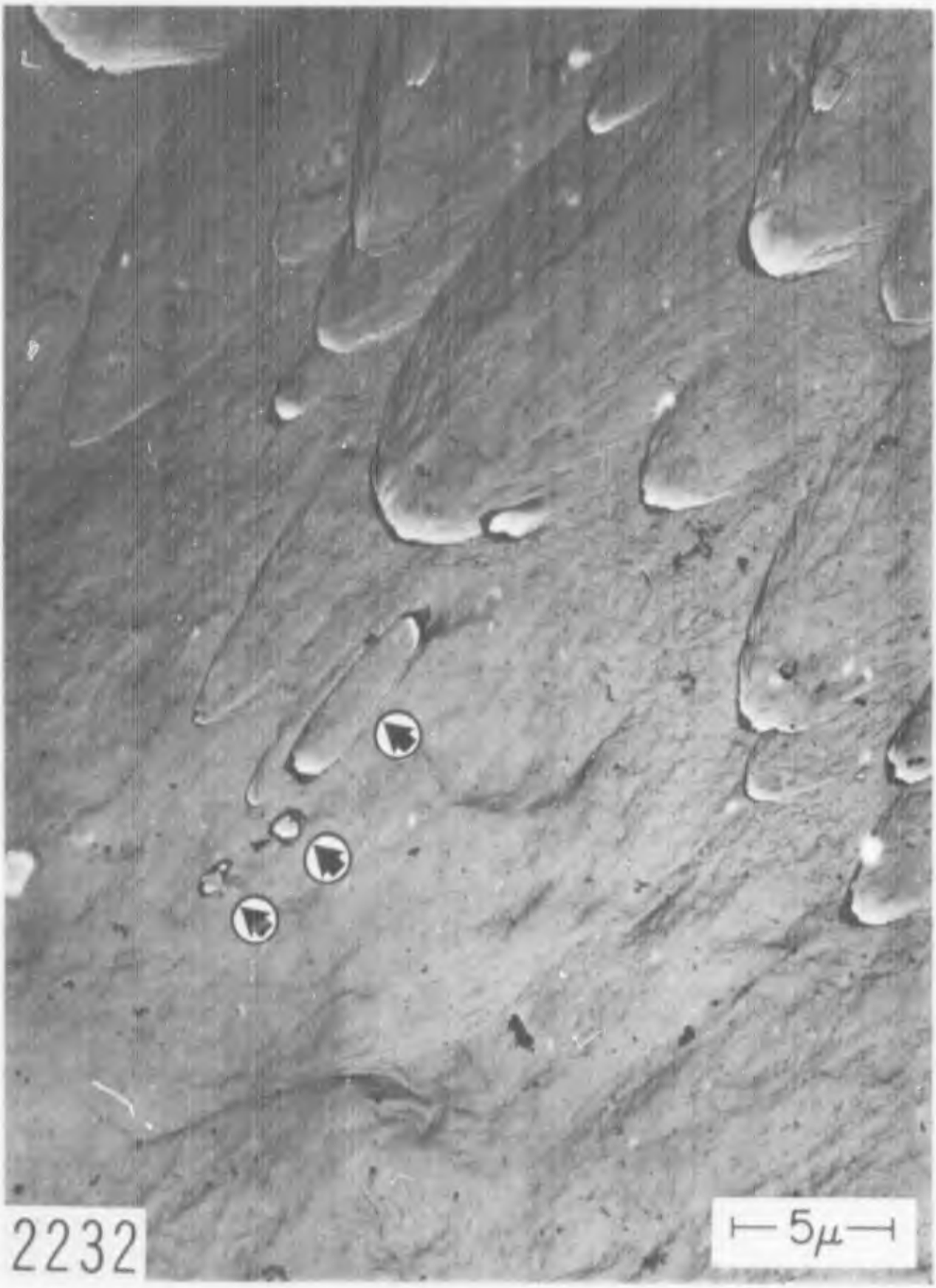

Fig. 16 - Stretched regions, shear dimples and oval tear dimples (arrows) in AISI 304 stainless steel. Palladium-shadowed direct carbon replica.

Fig. 17 - Examples of serpentine glide in dimples in tough pitch copper. Specimen alligatored due to residual stresses from rolling. An equiaxed dimple is shown by the horizontal arrow. Tear dimples are shown between slanted arrows. Palladium-shadowed direct carbon replica. 5000X.

Fig. 18 - Tear dimples in a hardened and tempered type 410 stainless steel specimen. Fracture propagated from lower right to upper left. Oval tear dimples are pointed out by arrows. Palladium-shadowed direct carbon replica. 2250X.

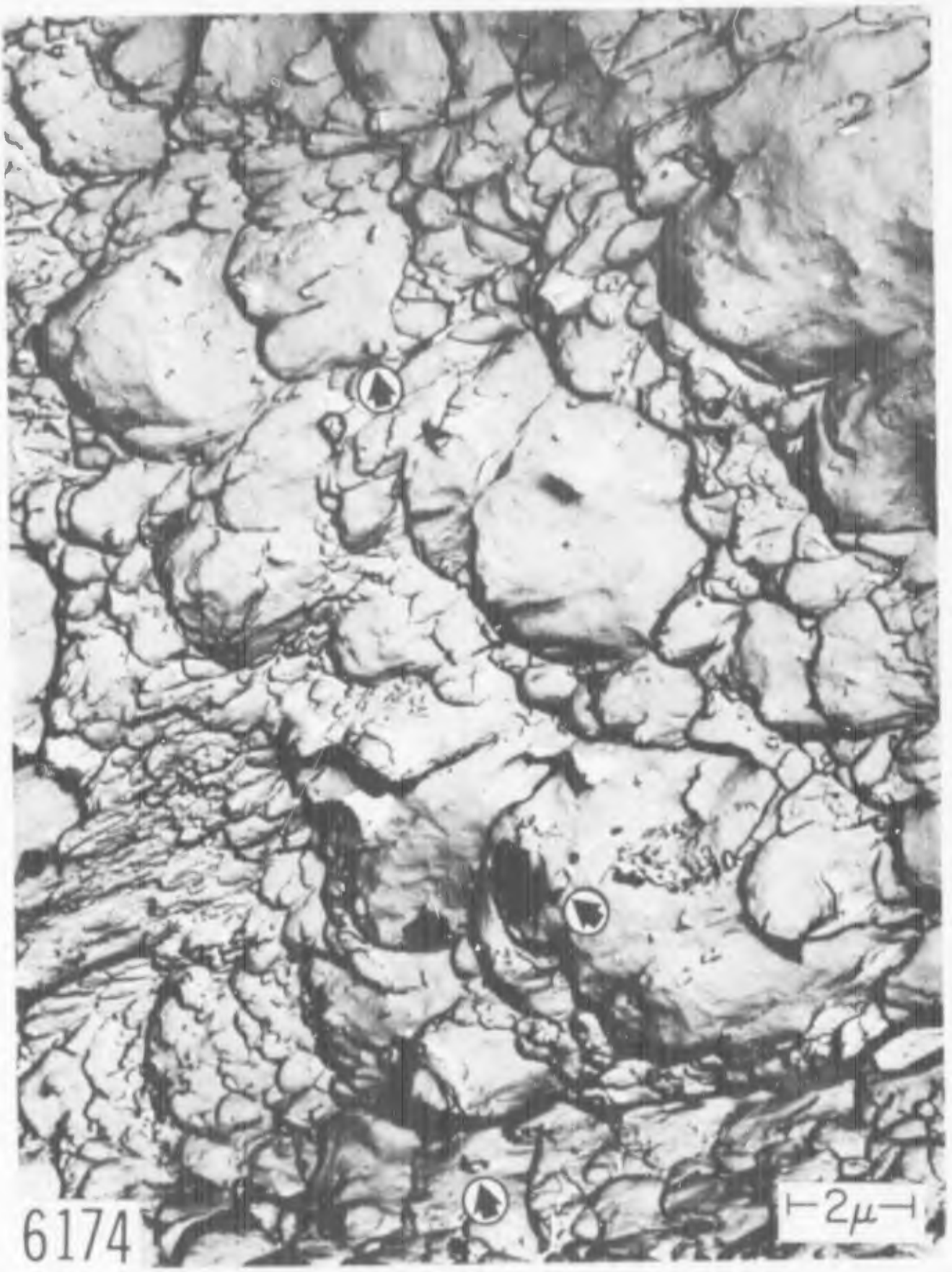

Fig. 19 - Tear dimples formed during the early stages of internal fracture of a hardened and tempered AISI 4340 smooth tensile test specimen broken in tension. Oval tear dimples are shown by arrows. Palladium-shadowed two-stage carbon replica. 12,000X.

Fig. 20 - Macroscopic view of AISI 4340 cup-and-cone fracture surface from which the fractograph in Fig. 19 was made. Fracture initiation region may be seen just above the center of the fracture surface. 4X.

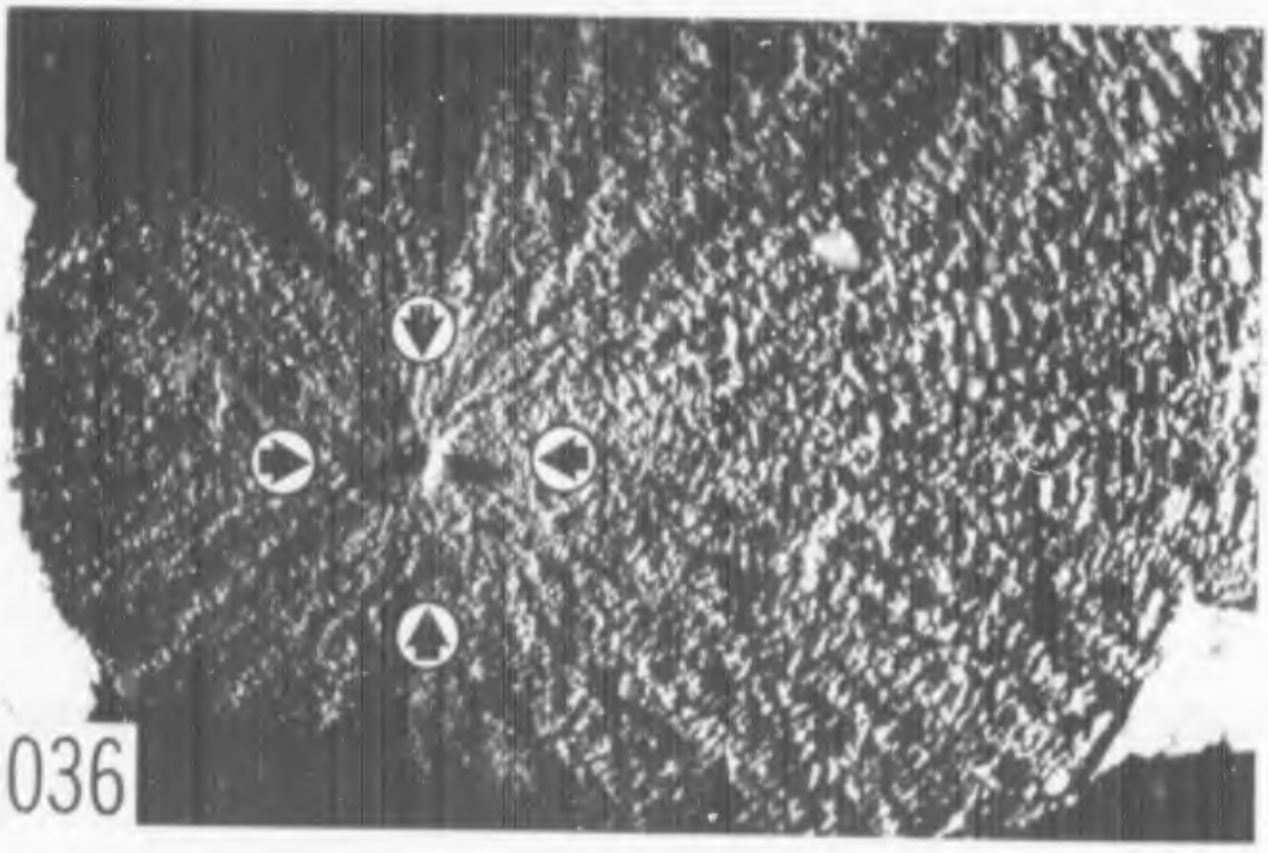

Fig. 21 - Closer view of "pinhole" fracture initiation region. Tearing was found in the central region bounded by the arrows. 35X.

Fig. 22 - Equiaxed dimples in a maraging steel. Two-stage palladium-shadowed carbon replica. 2100X.

Fig. 23 - Equiaxed dimples in AMS 6434. Two-stage palladium-shadowed carbon replica. 6000X.

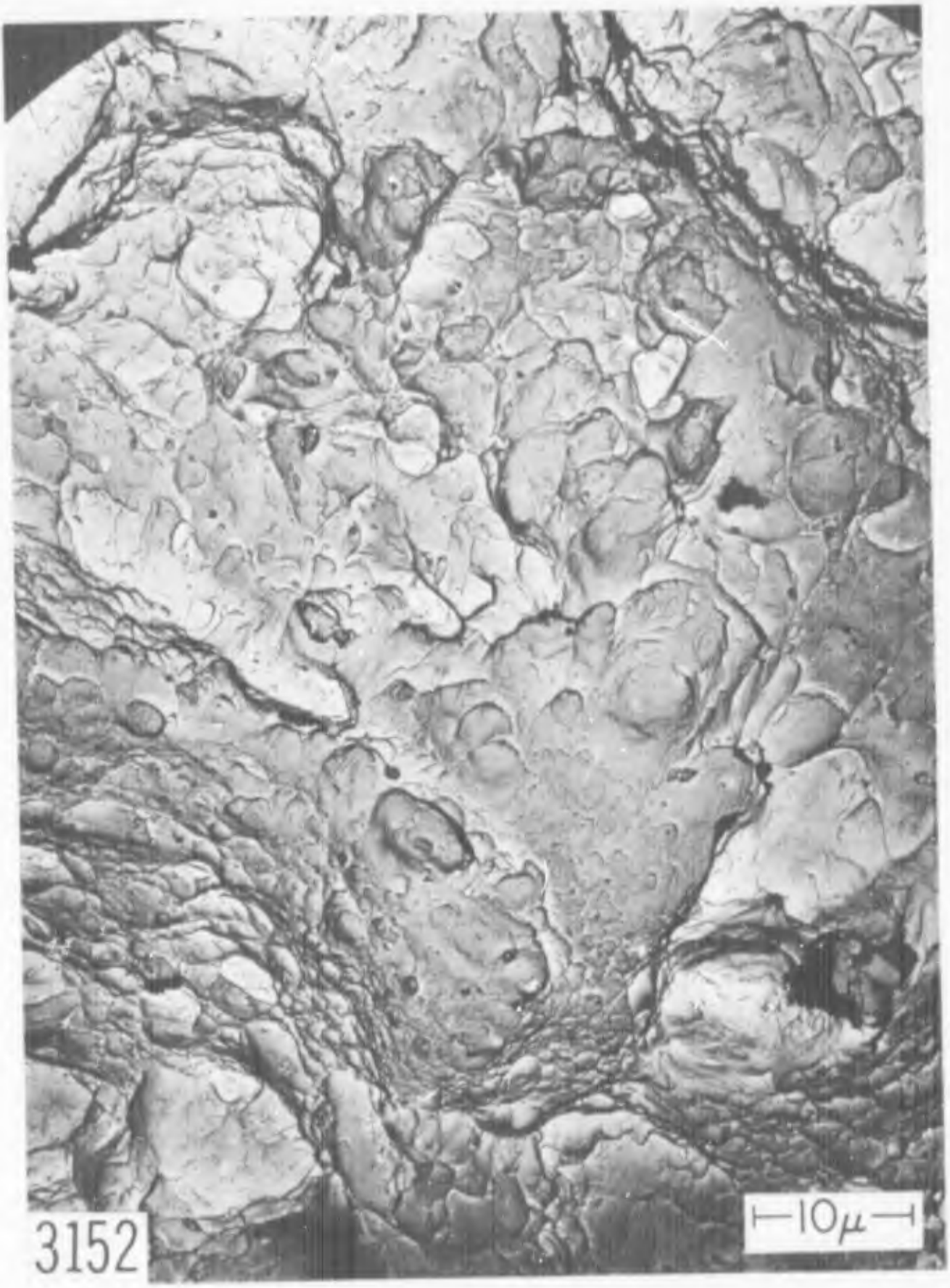

Fig. 24 - Equiaxed dimples in AISI 4338 steel. Two-stage palladium-shadowed carbon replica. 3000X.

Fig. 25 - Equiaxed dimples in a hardened and tempered low alloy steel specimen. Palladium-shadowed two-stage carbon replica. 6000X.

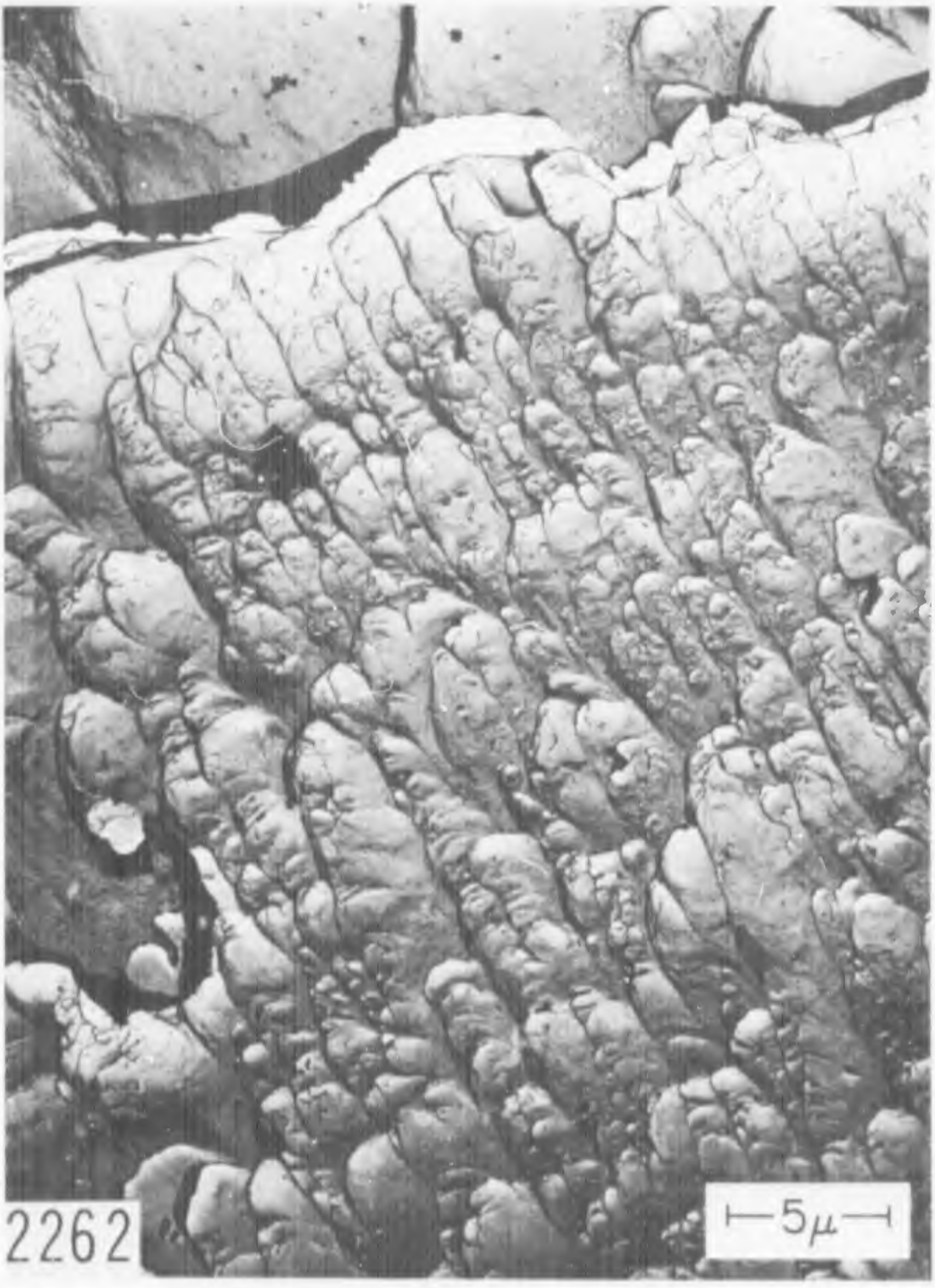

Fig. 26 - Shear rupture dimples in AISI 304 stainless steel "scab" formed by hypervelocity impact. Palladium-shadowed direct carbon replica. 6000X.

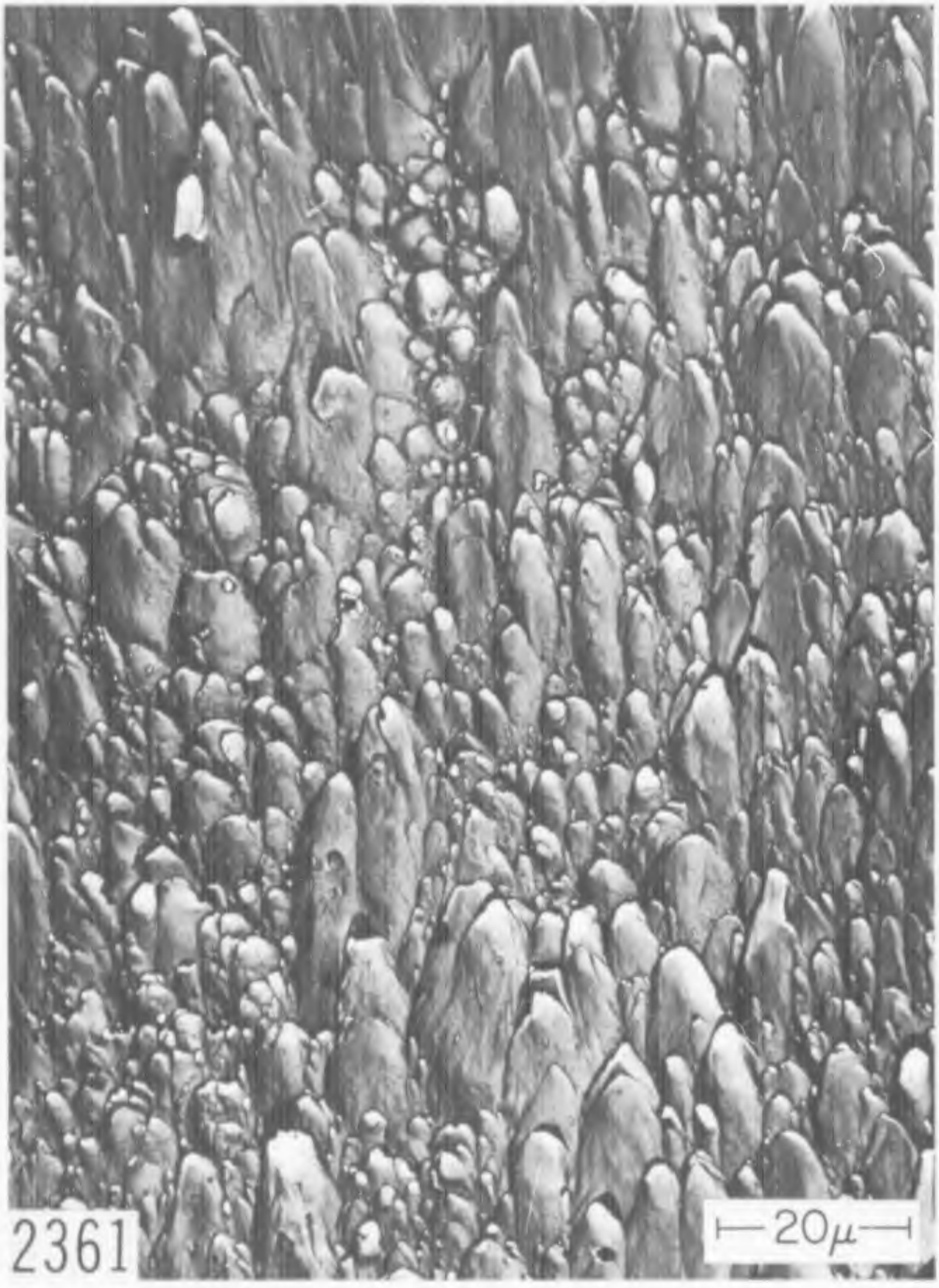

Fig. 27 - Shear rupture dimples in hardened and tempered Type 410 stainless steel. Palladium-shadowed direct carbon replica. 1800X.

Fig. 28 - Shear rupture dimples in Ti-4Al-3Mo-1V. Palladium-shadowed two-stage carbon replica. 2200X.

Fig. 29 - Shear rupture dimples on two sides of a quasi-cleavage facet. The arrows indicate shear dimples that have mates in Fig. 30. Material is hardened and tempered 410 stainless steel. Palladium-shadowed two-stage carbon replica. 3500X.

Fig. 30 - Fracture surface which matches that shown in Fig. 29. Same replicating conditions. 3500X.

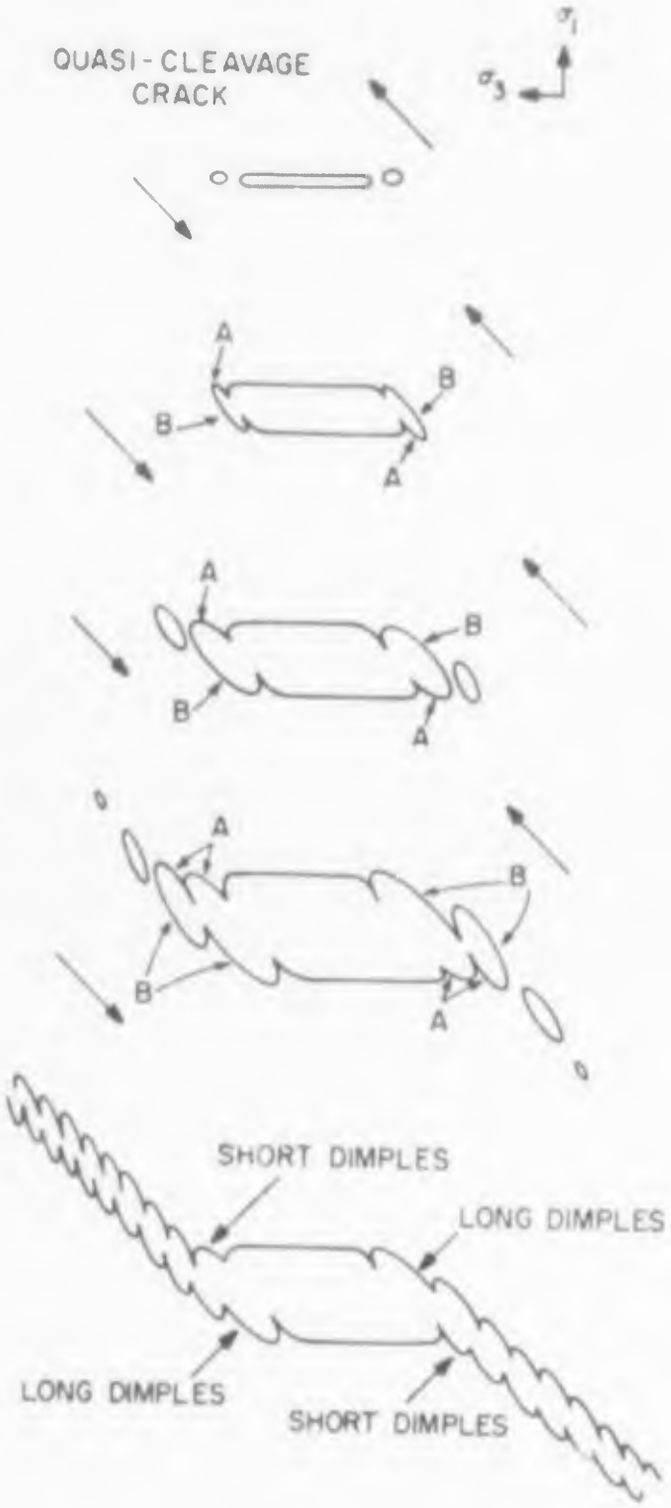

Fig. 31 - A simplified model of the formation of the shear rupture dimples shown in Figs. 29 and 30. A slightly opened quasi-cleavage crack is shown at top, and successive stages of shear rupture are illustrated in the lower sketches. The macroscopic principal stresses are shown at the top. Arrows on either side of the crack indicate shear directions. Dimples are stretched more at points B than at points A, particularly after the voids have started to coalesce with the advancing shear rupture crack.

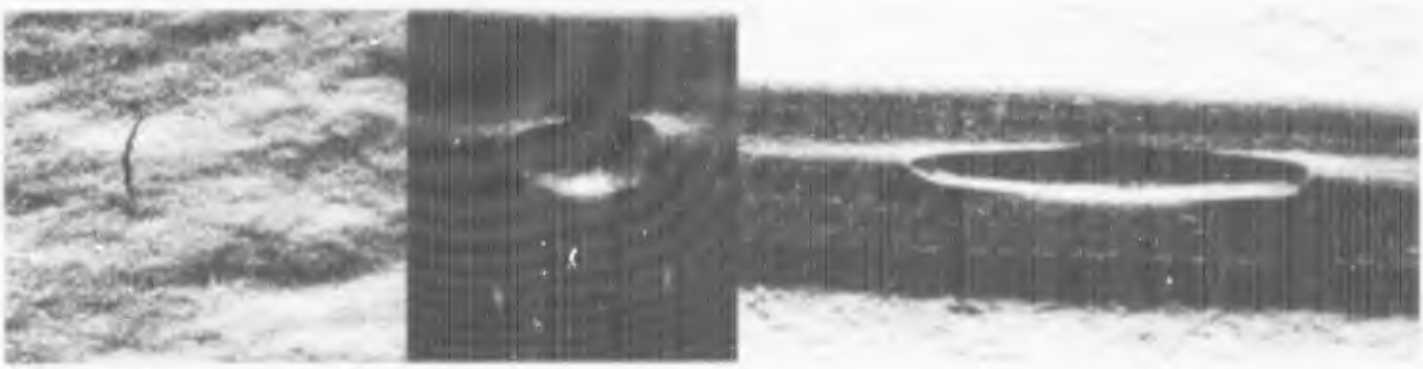

Fig. 32 - A rubber model demonstrating how a tear dimple stretches into an oval shape after the void coalesces with another free surface. The model is a rubber band, sliced part-way through the thickness with a razor blade, and then stretched.

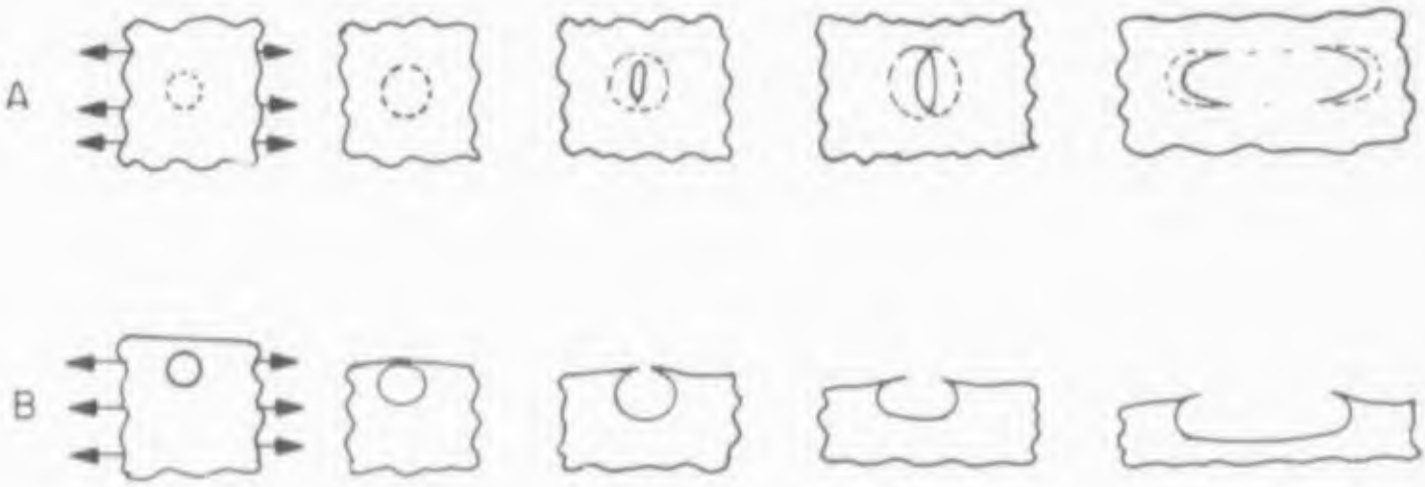

Fig. 33 - Sketch of the coalescence of a void with a larger free surface. The arrows indicate the direction of principal strain. The fracture surface is seen in (A) and the corresponding cross-sections of the void are seen in (B). Plastic deformation increases from left to right.

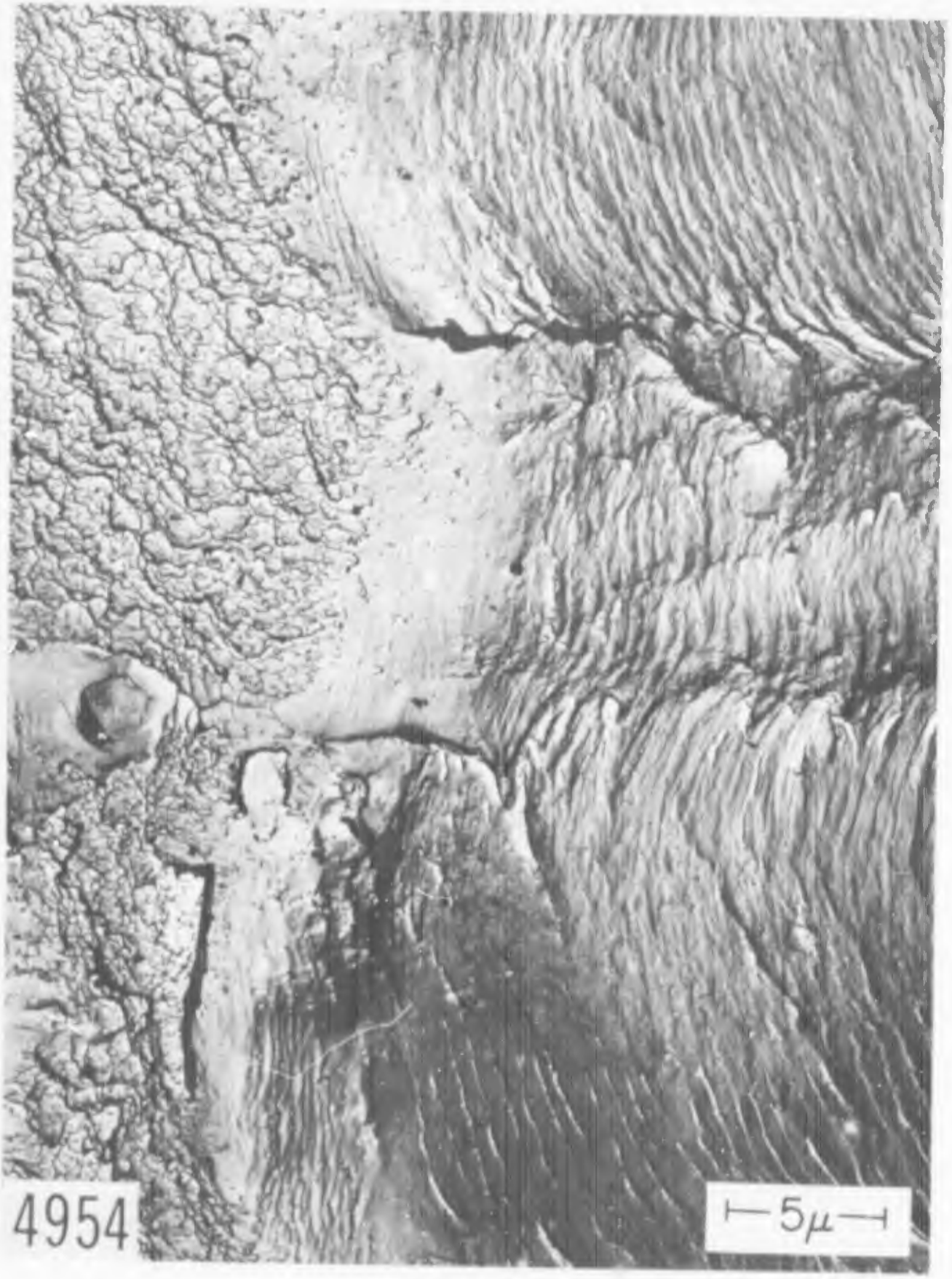

Fig. 34 - Stretching, glide plane decohesion and tearing at the tip of a fatigue crack. The fatigue crack was introduced into this 7075 T-6 aluminum alloy specimen as a stress raiser for the monotonic test which later produced the plastic rupture. Palladium-shadowed two-stage carbon replica. 6000X.

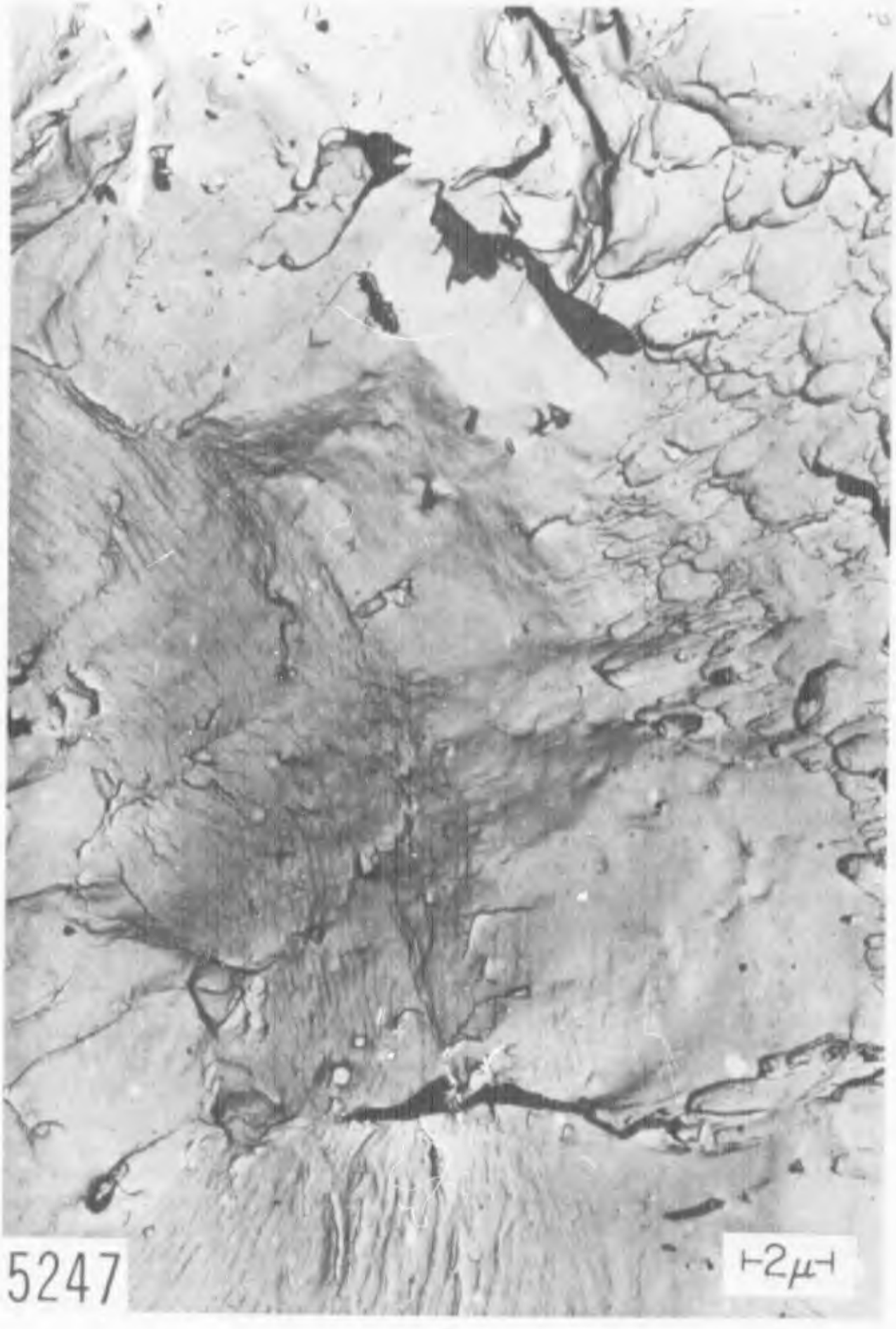

Fig. 35 - Another view of the intersection of a stress-raising fatigue crack with the monotonic fracture. Fatigue may be seen to the lower left. Stretching is followed by tearing during the test. Palladium-shadowed two-stage carbon replica. 9000X.

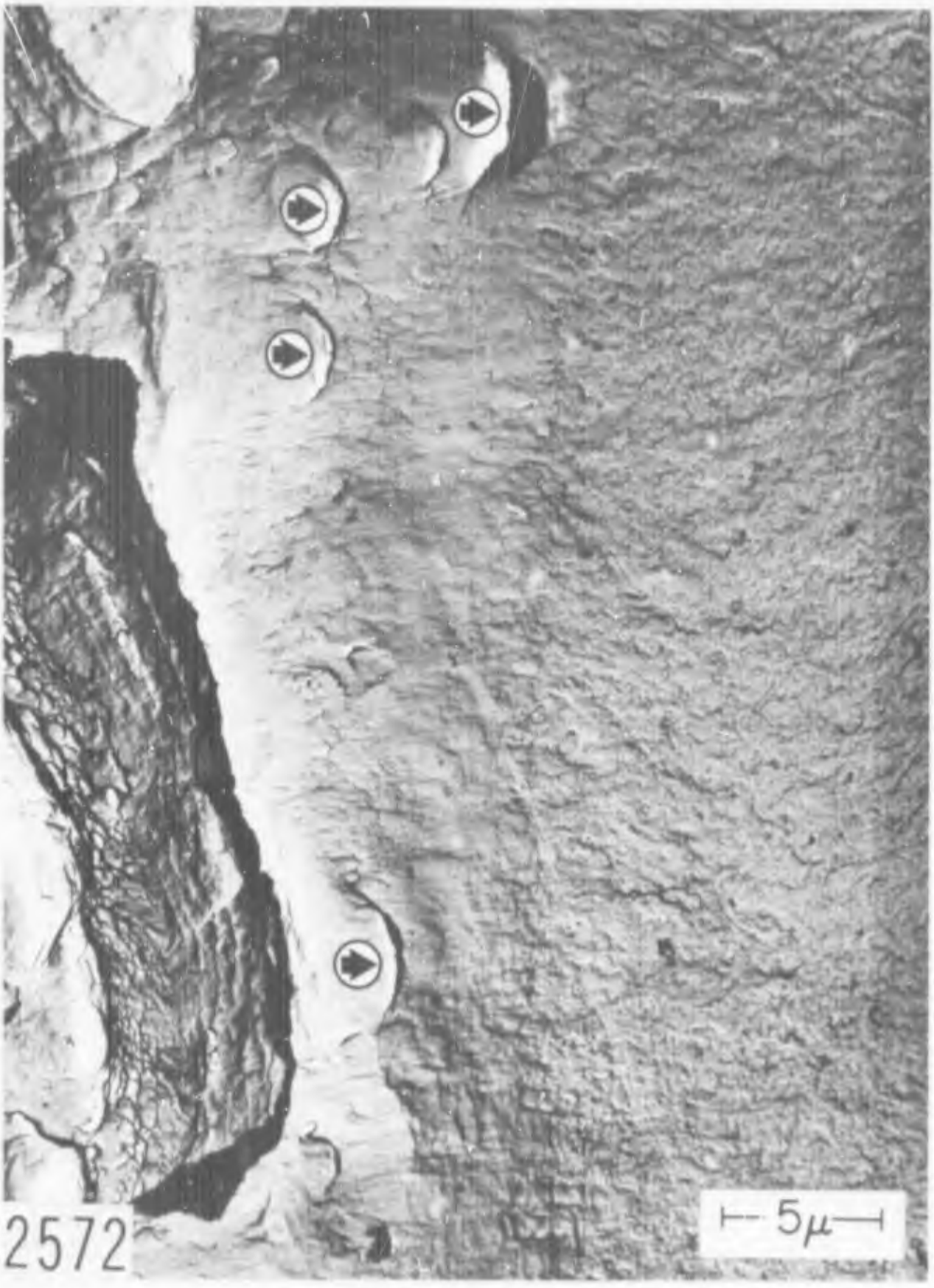

Fig. 36 - Stretching and tearing (arrows) at the tip of a fatigue crack in a Ti-2.5Al-16V specimen. Fatigue crack is to the right. Palladium-shadowed direct-carbon replica. 6000X.

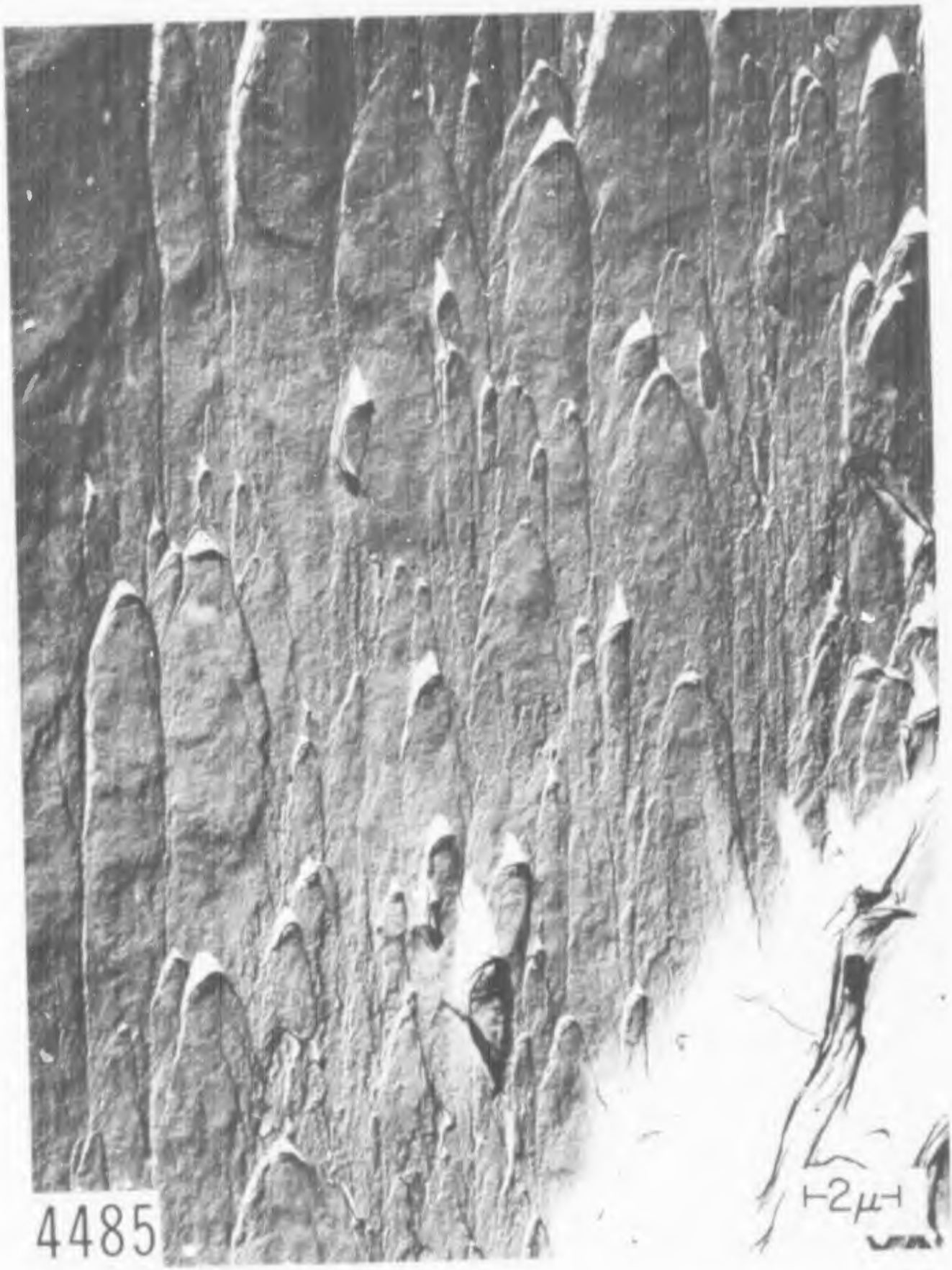

Fig. 37 - Long shear rupture dimples in an OFHC copper torsion rupture surface. Two-stage palladium shadowed carbon replica. 9000X.

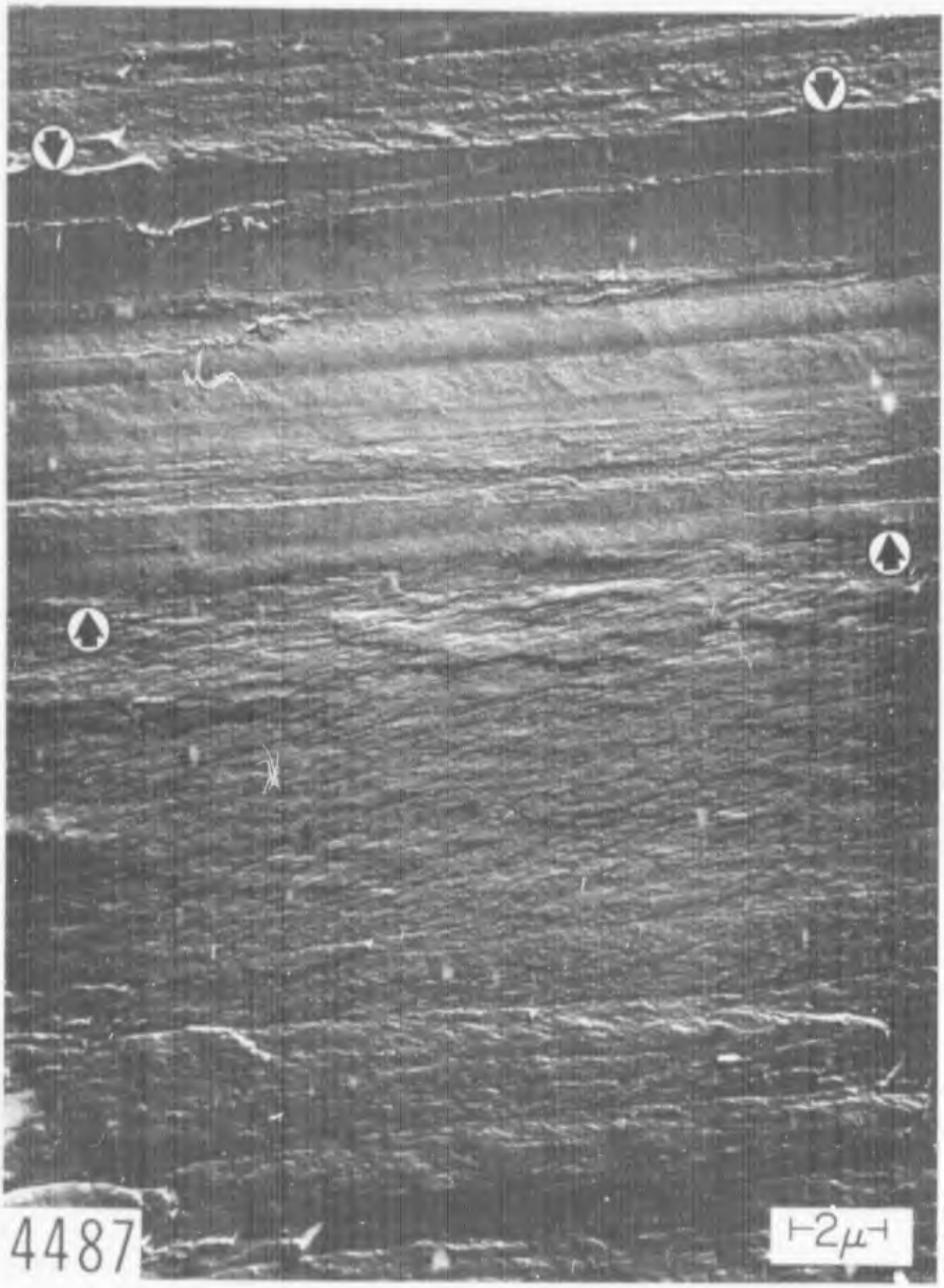

Fig. 38 - Long dimples (at bottom), burnishing markings (band near the top between arrows), and a region between of either burnishing or extreme stretching. Surface created in OFHC copper at the periphery of a torsion specimen. Two-stage palladium-shadowed carbon replica. 9000X.

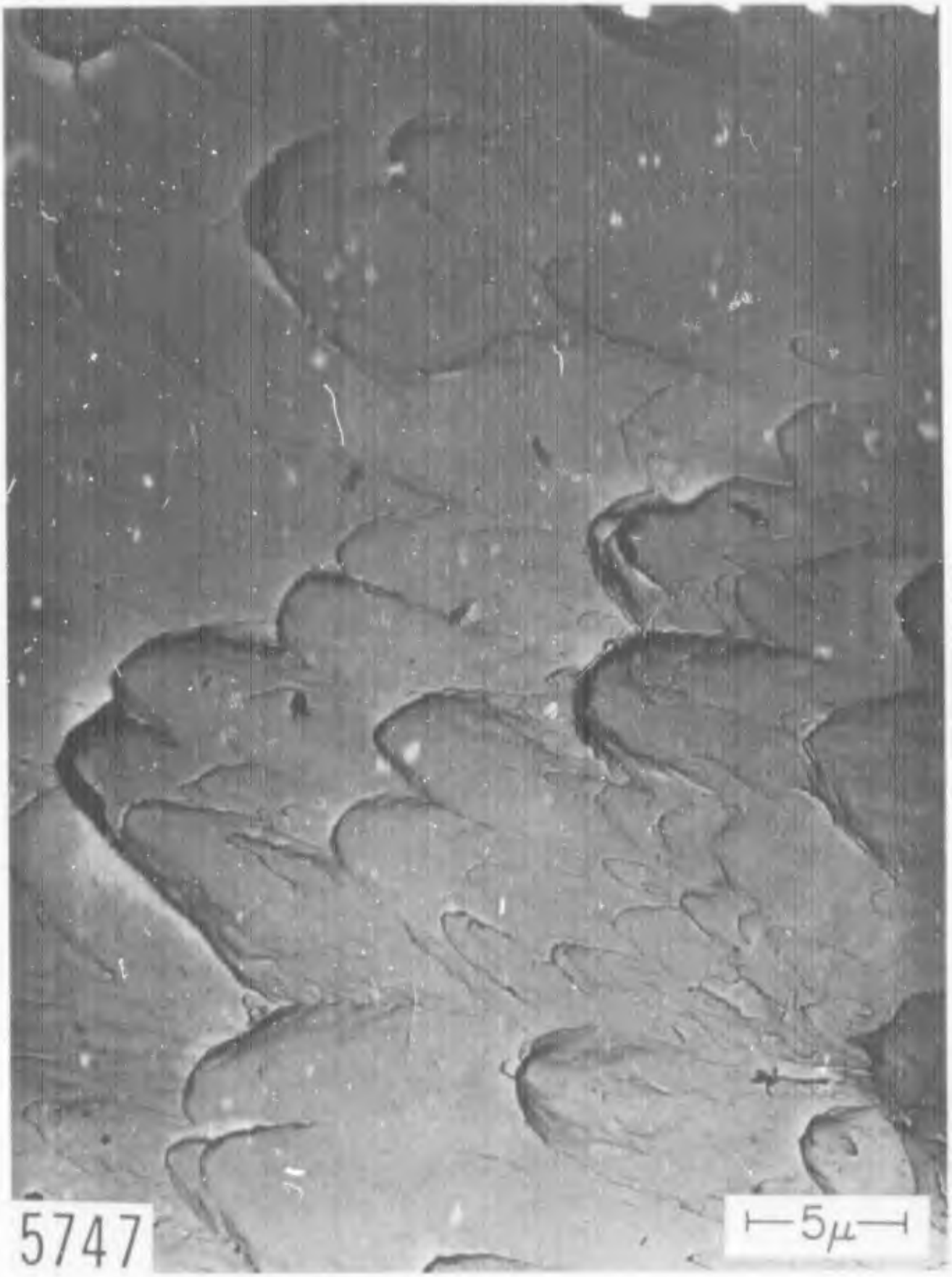

Fig. 39 - Shear rupture dimples in 99.999% Cu. These dimples were formed by lightly rubbing two mechanically polished surfaces together, causing friction welding and subsequent rupture. Two-stage palladium-shadowed carbon replica. 6000X.